MEDDELELSER OM GRØNLAND
UDGIVNE AF
KOMMISSIONEN FOR VIDENSKABELIGE UNDERSØGELSER I GRØNLAND
BD. 196 · NR. 4

GRØNLANDS GEOLOGISKE UNDERSØGELSE
BULLETIN NO. 108

THE FISKENÆSSET COMPLEX, WEST GREENLAND

PART II.
GENERAL MINERAL CHEMISTRY FROM QEQERTARSSUATSIAQ

BY

B. F. WINDLEY AND J. V. SMITH

WITH 34 FIGURES AND 10 TABLES

KØBENHAVN
C. A. REITZELS FORLAG
BIANCO LUNOS BOGTRYKKERI A/S
1974

Abstract

Electron microprobe analyses of 10 metamorphic mineral phases are given for rocks arranged in stratigraphic order through the Fiskenæsset "intrusion": 2 garnets, 11 olivines, 16 orthopyroxenes, 9 clinopyroxenes, 38 hornblendes, 8 phlogopites, 24 plagioclases, 6 spinels (pleonaste), 7 chromites and 7 magnetites. The element contents in minerals plotted with respect to zonal position in the intrusion and the inter-element distributions within minerals and between coexisting minerals suggest that the original igneous crystallization pattern of this gravity-differentiated, layered body has been only partly modified by metamorphic re-equilibration under hornblende granulite to high amphibolite facies conditions. Some igneous cryptic chemical variations are preserved in olivine, orthopyroxene, hornblende, plagioclase and magnetite, some leuco-gabbros retain their igneous cumulus plagioclase megacrysts, and rare ultramafics retain their igneous olivine, orthopyroxene, clinopyroxene, and hornblende primocrysts. Chemical migration of elements within and amongst grains during the metamorphism appears to have been small, so that the present minerals have a mixture of both igneous and metamorphic characteristics.

ISBN 87 421 0093 3

CONTENTS

INTRODUCTION AND REGIONAL GEOLOGICAL SETTING

The Fiskenæsset "complex" is situated in the early Precambrian central basement block of West Greenland. It consists of a metamorphosed layered "intrusion" with well-preserved igneous stratigraphy bordered by meta-volcanic amphibolites into which it was emplaced.

The first paper of this series on the complex (WINDLEY *et al.*, 1973) describes its stratigraphy and petrology and presents preliminary whole-rock chemical data. This second paper is based on electron microprobe analyses of minerals.

It was inferred that the intrusion was infolded with the basic volcanic rocks into an underlying gneissic basement. The cover–basement units were tectonically interleaved so that all rock groups became mutually conformable; they were variably recrystallized by granulite- and amphibolite-grade metamorphisms, and were folded several times. The Fiskenæsset intrusion now occurs, therefore, as a concordant layer up to 2 km thick in granitic gneisses, bordered by its meta-supracrustal amphibolites with minor marbles and schists. In spite of subsequent deformation and metamorphism the complex still extends as a virtually unbroken folded layer for at least 200 km (strike length) and much of its igneous history is still decipherable.

The Pb/Pb age of the late granulite facies metamorphism is calculated at 2900 m.y. (BLACK, L. P., MOORBATH, S., PANKHURST, R. J. & WINDLEY, B. F., 1973) and the Rb/Sr whole-rock isochron age at 2850 m.y. (EVENSON & MURTHY, pers. comm.).

SUMMARY OF THE MAIN FEATURES OF THE FISKENÆSSET COMPLEX

The Fiskenæsset complex as seen on the island of Qeqertarssuatsiaq (fig. 1) is subdivided into zones which have been so intensely thinned and thickened by deformation that it is difficult to find them all in any one traverse across the strike. However, it has been possible to make the

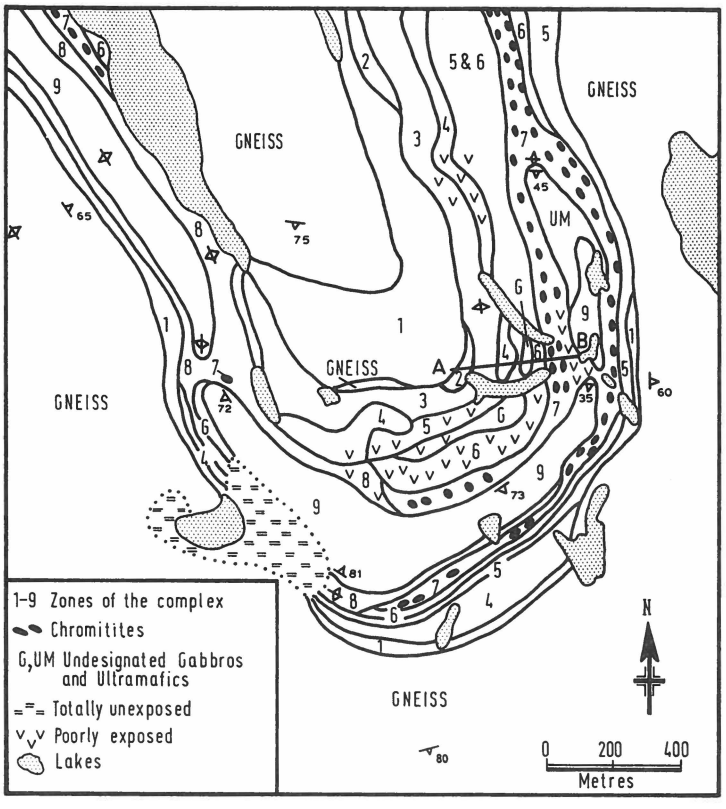

Fig. 1. Map of the Fiskenæsset complex in south central Qeqertarssuatsiaq showing the main zones. The line A–B gives the position of most of the samples mentioned in fig. 2.

following maximum stratigraphy by bulking information from several areas:

		Major zones	Max. thickness (metres)
Top	9	Pyroxene amphibolite	50
	8	Garnet anorthosite	75
	7	Major chromitite	20
	6	Anorthosite	130
	5	Homogeneous leuco-gabbro with marked cumulate texture	250
	4	Dark gabbro	60
	3–4	(Minor chromite-bearing gabbros and orthopyroxenites)	10
	3	Layered leuco-gabbro with anorthosite laminae	100
	2	Magnetite-rich layered ultramafics (pyroxenites, peridotites, dunites)	100
Bottom	1	Pyroxene amphibolite	200

Zones 2–8 make up the intrusion and were formed by gravity differentiation. Zones 1 and 9 comprise metamorphosed basic volcanic rocks within which the intrusion was emplaced. The lower half of the intrusion is largely mafic and ultramafic and the upper half anorthositic. A minor chromiferous sub-zone between zones 3 and 4 is referred to as zone 3–4 for convenience.

The complex was deformed into an isoclinal syncline, presumably when infolded into its gneissic basement, with the result that the above stratigraphy in the Fiskenæsfjorden area is repeated symmetrically in reverse order, the upper zones being innermost (fig. 1).

Preliminary whole-rock analyses (WINDLEY *et al.*, 1973) show that the differentiation data of the two "halves" of the intrusion mirror each other reflecting the symmetrical stratigraphy. The Fe/Mg ratio, which best defines the course of crystallization of the intrusion, and the contents of Al_2O_3, $Na_2O + K_2O$, and total normative feldspar increase upwards from zones 2 to 8, whilst MgO + FeO, Co and the normative colour index show a corresponding decrease. The fact that the differentiation trend, which displays non-iron enrichment, is preserved means that the granulite facies metamorphism was essentially isochemical.

From petrographic and whole-rock chemical data it was concluded that the original magma had a high water content which was responsible for the following mineralogical and chemical features: amphibole crystallized as a stable primocryst phase, the accumulation of plagioclase was delayed enabling it to concentrate as late anorthosite, and the amount of plagioclase relative to ferromagnesian minerals was increased causing the formation of thick anorthosites. The high oxidation state of the magma also gave rise to a non-iron enrichment differentiation trend; in so far as the intrusion displays decrease in total iron with progressive fractionation, it is dissimilar to the Skaergaard, Bushveld and Stillwater complexes formed from anhydrous magmas.

From petrographic examination of the highest grade mineral assemblages preserved in the intrusion it is suggested that the following mineral assemblages made up the igneous rock suite:

Anorthosites and leuco-gabbros: plagioclase + orthopyroxene ± clinopyroxene ± hornblende ± spinel.
Gabbros and norites: plagioclase + orthopyroxene ± clinopyroxene ± hornblende ± spinel ± other oxides.
Chromitites: chromite ± orthopyroxene ± hornblende ± rutile.
Dunites: olivine ± hornblende ± spinel ± sulphides and other oxides.
Pyroxenites: orthopyroxene ± clinopyroxene ± hornblende ± spinel ± sulphides and other oxides.
Peridotites: olivine + orthopyroxene ± clinopyroxene ± hornblende ± spinel ± sulphides and other oxides.

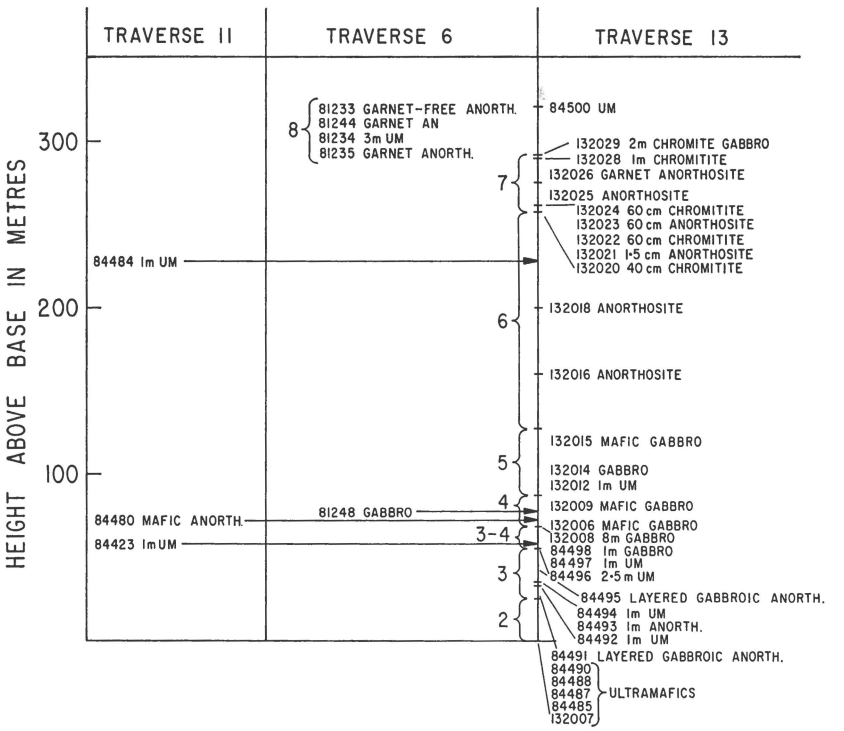

Fig. 2a.

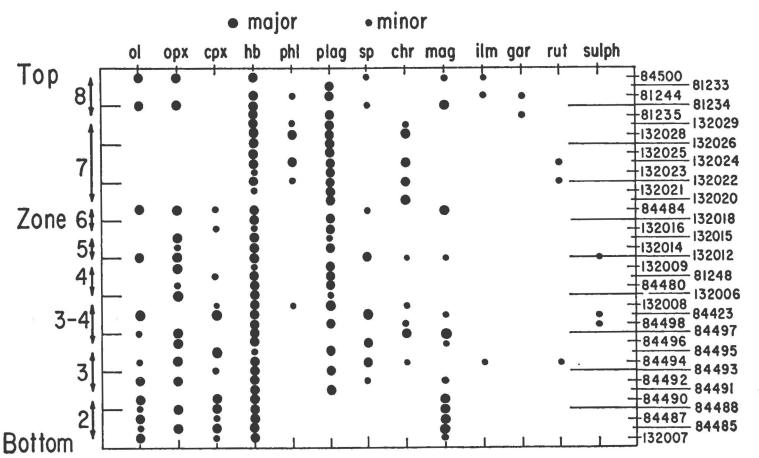

Fig. 2b.

Fig. 2. Stratigraphic location (a) and mineralogy (b) of rocks analyzed in this study. For regional location of traverses 6, 11 and 13 see WINDLEY *et al.* (1973). The abundance of the minerals in (b) was estimated visually from thin sections.

These minerals were variably recrystallized to metamorphic counterparts during high-grade metamorphism. Some relict igneous primocrysts are preserved such as plagioclase in gabbros and leuco-gabbros, and olivine, pyroxenes and hornblende in zone 2 ultramafics.

The present paper describes a reconnaissance of the metamorphic mineralogy using electron microprobe analyses. Details of the relict igneous mineralogy of some samples from zone 2 will be given in a later paper, and will be used as a basis for detailed interpretation of the primary mineralogy of the intrusion. The present paper contains analyses of several minerals (e.g. olivines) from rocks in zone 2 which retain at least some of the primary igneous mineralogy, but the main burden of the paper is on the metamorphic mineralogy. Various other aspects will be reported later, including a detailed study of the opaque minerals.

Most of the samples used in the present study were collected in stratigraphic order from one traverse across the complex shown in fig. 1, which is close to the traverse where the analysed whole rock samples of WINDLEY *et al.* (1973) were taken. This sampling area was chosen on account of the 1 km thickness of the complex (a major fold core) and its relatively high metamorphic grade (surrounding gneisses show evidence of granulite facies metamorphism). A few additional samples were selected from two other traverses (fig. 2a). The mineral assemblages of all the numbered rock samples used in this study are given in fig. 2b. It should be noted that the rock samples were not collected at equal distances in the field, but were chosen to be representative of the stratigraphic variations throughout the complex. The height of the samples above the base of the complex is shown in fig. 2a. Note that the double-arrows on figs 2b and 3 do not correspond to the thickness of the zones.

ELECTRON-MICROPROBE TECHNIQUE

The technique was deliberately chosen to give reconnaissance analyses of moderate accuracy and high speed. High accuracy, especially for minor elements, requires considerable time and was not necessary for this initial study. Future specialized studies will provide higher accuracy, and will probably utilize both electron and ion probe techniques in order to cover trace elements as well as minor and major elements. Compilers of tables of mineral analyses are warned specifically not to regard the present data as representing the best possible results.

All analyses were made on polished thin sections using the general technique of SMITH (1965) on an ARL–SM electron microprobe. Corrections were made with the EMPADR VII program of RUCKLIDGE (1967). Standards for the silicate minerals were: synthetic plagioclases (Lindsley); Kokomo sanidine (for K); synthetic diopside

(Schairer); Eskola 21 and 400 orthopyroxenes; synthetic Di2Ti and Di,Na glasses (Boyd); Turkevich olivine (for Ni); Mn-hortonolite, Hess 1 (for Cr) and a natural apatite (for P). For the spinel group of minerals and the ilmenites only rudimentary calibrations were made for the major elements but the minor elements were calibrated with the same standards used for the silicates.

The spectrometers of an ARL electron microprobe can be reset from the wavelength dials with a reproducibility of peak intensity that ranges from about 3 to 7 % in standard deviation depending on the type of analyzing crystal. This poor reproducibility results from mechanical problems and requires frequent resort to standards if one wishes to attain high accuracy (about 1 %). For our reconnaissance studies we deliberately adopted the following procedure which gives high relative accuracy for the major elements (1 % of the amount present) and low relative accuracy for the minor elements (*c.* + 5 % of the amount present).

For each chosen mineral grain on a polished thin section, a wavelength sweep was made yielding a high and low background plus at least two peak readings for the elements Na, Mg, Al, Si, P, K, Ca, Ti, Cr, Mn, Fe and Ni. A spot size of 5 to 10 μm was used, and the two or more peak readings were taken on different parts of the grain, one near the center and one near a margin. If they differed by more than two standard deviations of the counting statistics, further readings were taken to check for accidental impurity or extensive zoning. Nearly all grains were essentially homogeneous chemically, except for occurrence of amphibole (?) inclusions in some plagioclases and exsolution lamellae in some pyroxenes. These inclusions need further investigation. The positions of the analytical points were recorded using the *XY* dials. At the completion of all the wavelength scans, the major elements were reanalyzed using fixed wavelength comparison between standards and unknowns.

All analyses were made at 15 kv, and the beam current was high enough to give a sensitivity of about 0.01 to 0.02 wt. % for the minor elements. Unfortunately this results in count rates up to 10000 counts per second for some major elements with possible errors in correction for dead-time. After completion of the work it was found that one of the counters had lost its linearity, but the likely error was believed to be around 1 to 2 % for the major elements. Unfortunately several specimens were accidentally analyzed using standards sputtered on a separate occasion. The small difference of thickness of carbon coat results in oxide totals several per cent from the theoretical value. An arbitrary correction was applied evenly to all the elements as specified in the tables.

Generally speaking the present analyses should be accurate to within 3 % of the amount present for most major elements and 7 % of the amount present for most minor elements (except for very low concentrations where an absolute error near 0.02 % acts as an asymptotic limit).

For plagioclase, a few tests showed that the minor element content was rather low. Consequently most plagioclase analyses were obtained by using fixed wavelengths for Ca, Na and K. Most samples showed little if any evidence of chemical zoning, and no attempt was made to obtain detailed compositional profiles.

MINERAL CHEMISTRY

The microprobe analyses recalculated from metal to oxide are given at the end in tables 1 to 10 labelled *a*. Tables labelled with *b* show atomic contents calculated to the number of oxygens used by DEER, HOWIE &

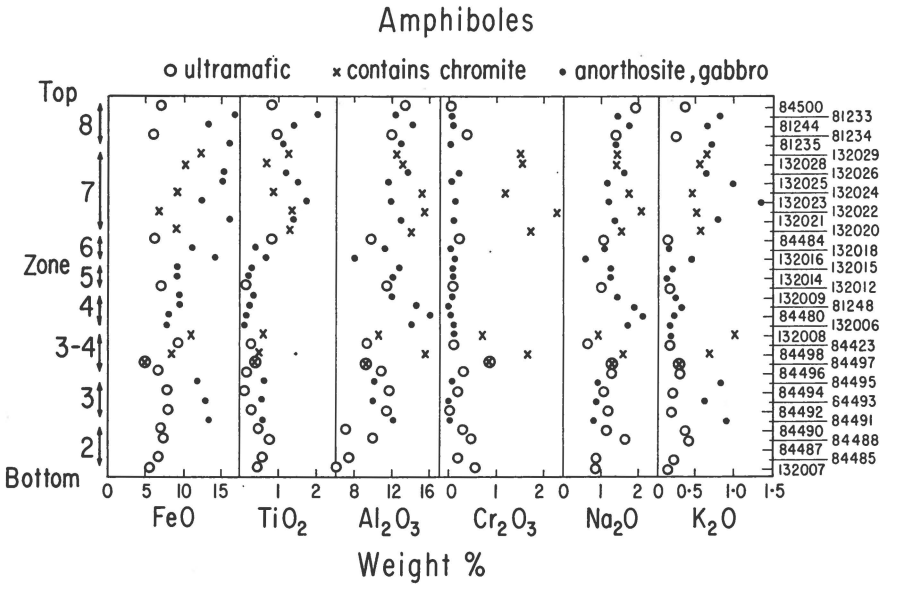

Fig. 3. Variation with zonal sequence of the composition of amphiboles. The rocks were split into three groups: ultramafic, anorthosite plus gabbro, and those containing chromite. One ultramafic rock, 84497, contains scattered grains of chromite. Note that for Al_2O_3 and Cr_2O_3, zero wt. % does not correspond to the left-hand boundary.

Zussman (1963). Since the electron microprobe yields only total Fe, the iron was assumed to be entirely in the ferrous state for the initial calculation. For the garnets the effect of assuming 5 % Fe as ferrous is shown. For the spinel and chromite minerals an arbitrary split into the ferrous and ferric states was made in order to minimize the deviation of the sums of the tetrahedral and octahedral cations from the ideal values: of course, such a calculation is highly inaccurate.

The minerals will now be discussed in the order used by Deer *et al.* (1963), except that amphibole will be treated first since it is the commonest mineral occurring in all the zones.

Amphibole. All the amphiboles can be broadly described as hornblendes. Because of the complexity of the substitutions it is difficult to depict the chemical variations.

Fig. 3 shows the variation of FeO, TiO_2, Al_2O_3, Cr_2O_3, Na_2O and K_2O with position in the complex. Each amphibole is marked with a symbol to show whether it derives from an ultramafic rock, or from a chromite-bearing rock, or from either a gabbro or an anorthosite. One ultramafic rock, 84497, contains rare, scattered grains of chromite and is denoted by a double symbol. At first sight, the data are almost random but detailed study reveals many facets.

The FeO content tends to be least in amphiboles from ultramafic rocks, highest for anorthosites and gabbros, and intermediate but erratic for chromite-bearing rocks. Fig. 4 shows that for the amphiboles of just the gabbros and anorthosites the wt. ratio MgO/FeO increases from zone 3 to zones 4 and 5 and then decreases to zone 8. Individual amphiboles give considerable scatter, but the averages for each zone can be represented nicely by a single peaked curve. Of course, the statistics are poor,

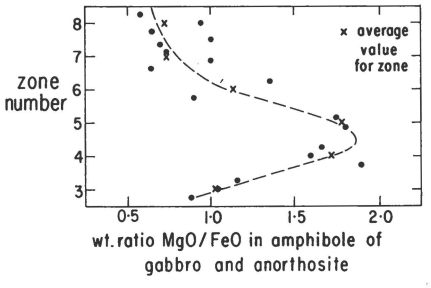

Fig. 4. Variation with zonal sequence of the wt. ratio MgO/FeO of amphiboles from the gabbros and anorthosites. The dashed line was estimated visually from the mean value (crosses) for each zone.

and the position of a rock in its particular zone is not precisely defined. For the amphiboles from the ultramafic rocks, it is clear from fig. 3 that there is a weak maximum in the FeO content at zones 3 and 4. A corresponding minimum in the MgO content also occurs but is not shown graphically. Thus the FeO content of the amphiboles from the ultramafic rocks varies antipathetically with that for the ones from the anorthositic and gabbroic rocks, as may be seen graphically in fig. 3.

The TiO_2 content of the amphiboles is highest in zones 7 and 8, irrespective of the host rock. There is a minor maximum in zone 2 for the amphiboles from ultramafic rocks. In general, the amphiboles from the anorthosite-gabbro rocks contain more TiO_2 than those from the ultramafics.

The Al_2O_3 contents vary greatly and there are no obvious patterns. In zone 2, the ultramafic rocks yield amphiboles with 7 to 10 wt. % Al_2O_3, whereas in the middle zones the spread is mostly between 10 and 15 wt. %.

The Cr_2O_3 content is very low for the amphiboles from all the anorthosite-gabbro rocks (note that the zero is deliberately displaced from the boundary in fig. 3). On the other hand, all the chromite-bearing rocks contain an amphibole rich in Cr_2O_3, the amount varying from 0.7 wt. % to over 2 wt. %. Clearly there is a sympathetic relation between the Cr content of the amphibole and the presence of chromite. (Since completion of these analyses, scattered small grains of chromite were

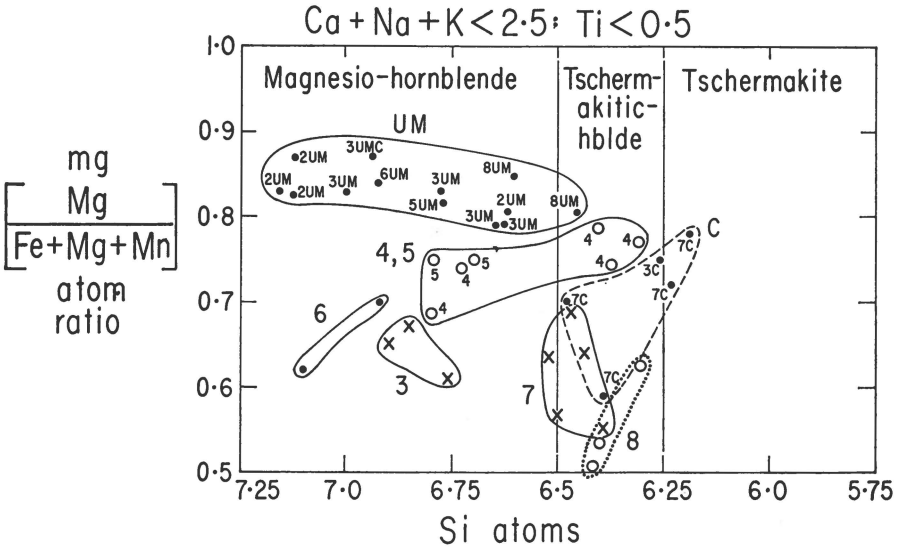

Fig. 5. Classification of the amphiboles with respect to a diagram given by LEAKE (1968). All the amphiboles have less than 2.5 atoms of (Ca + Na + K) and less than 0.5 atoms of Ti per 23 oxygen atoms in the water-free formula. The small numbers beside each point refer to the zone, and the capital letters refer to ultramafic (UM) and chromite-bearing (C) samples. The samples are grouped into seven ringed areas labelled by the large symbols.

found in 132012, whose amphibole is not Cr-rich). The amphiboles from the ultramafic rocks tend to contain more Cr_2O_3 than those from the anorthosite-gabbro rocks, with values rising to about 0.5 wt. % in zone 2.

The Na_2O content of the amphiboles is erratic, mostly lying between 1 and 2 wt. %, and perhaps tending to increase for higher zone numbers. There is no obvious difference in sodium content for the amphiboles from the different rock types. The K_2O content, however, does show a correlation, being lower in general for the amphiboles from the ultramafic than for the anorthosite-gabbro rocks.

Turning now to the detailed classification of the amphiboles, fig. 5 shows the analyses plotted on a diagram given by LEAKE (1968, fig. 2). This diagram applies to amphiboles with less than 2.5 atoms of (Ca + Na + K) per unit formula, and less than 0.5 atoms of Ti. The latter criterion is satisfied easily by all the Fiskenæsset amphiboles, while the former criterion is broken only by three amphiboles which contain only slightly more than 2.5 atoms of (Ca + Na + K). On this plot of *mg* atom ratio versus number of Si atoms, the Fiskenæsset amphiboles mostly fall in the areas assigned to magnesio-hornblende and tschermakitic hornblende, while two fall in the tschermakite region. None of the amphibole has an *mg* ratio below 0.5 which would require the addition of the prefix

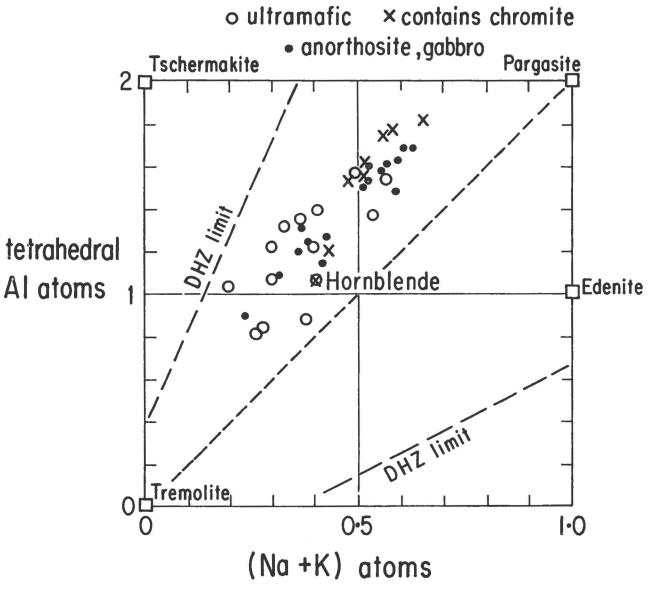

Fig. 6. Classification of the amphiboles with respect to fig. 71 of DEER *et al.* (1963, v. 2). The numbers of tetrahedral Al and of (Na + K) atoms are specified with respect to 23 oxygens in the water-free formula. The number of tetrahedral Al atoms is obtained by adding Al to Si until 8 tetrahedral atoms is reached. The symbols show the rock type: one ultramafic rock contains some chromite. The outer dashed lines show the limits of analyses plotted by DEER *et al.* while the central line merely joins tremolite to pargasite.

ferro. The term tschermakite, of course, implies the extensive substitution of aluminum thereby reducing the content of Si atoms.

From fig. 5 it may be seen that the amphiboles from the ultramafic rocks, irrespective of the zonal position are delineated from all the other amphiboles, being rich in *mg* and high in Si, thereby falling mostly in the field of magnesio-hornblende. The amphiboles from chromite-bearing rocks are lower in Si and *mg*, falling in the fields of tschermakite. All the remaining amphiboles are best characterized in terms of zonal position as shown by the respective areas in fig. 5. There is not a steady change of composition with increasing zone number, and it is obvious that the chemical composition of the amphiboles depends on more than one factor.

Fig. 6 shows the amphibole compositions plotted with respect to tetrahedral Al and (Na + K) atoms per unit formula. This plot may be compared with fig. 71 in DEER *et al.* (1963, v. 2) which has reference points for ideal tremolite, tschermakite, pargasite and edenite. The two outer dashed lines show the limits of the region populated by hornblendes. The Fiskenæsset amphiboles fall well inside this region somewhat biased towards the composition of tschermakite. There is strong overlap between

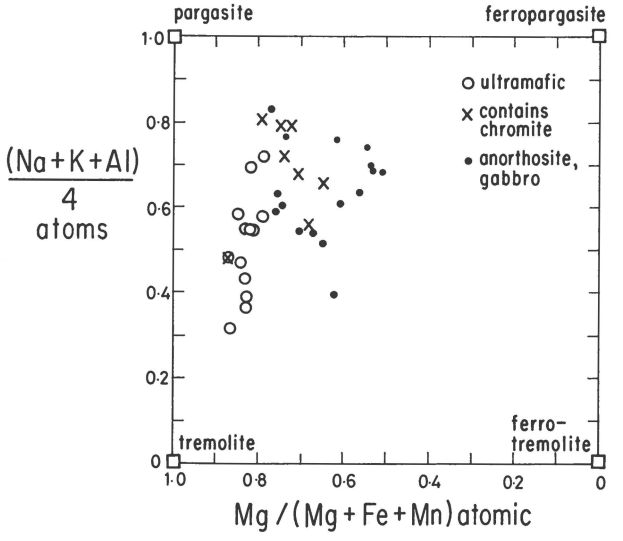

Fig. 7. Classification of the amphiboles with respect to fig. 10 of ERNST (1968). Since the electron-microprobe analyses did not yield the amount of ferric iron, this was omitted on the ordinate. Potassium was added to sodium so that the ordinate is (Na + K + Al) rather than (Na + Al + Fe^3) atoms per 4 formula units. For convenience the abscissa is given in terms of Mg ratio rather than Fe. The symbols show the rock type: one ultramafic rock contains some chromite.

the composition ranges of the amphiboles from ultramafic and the anorthosite-gabbro rocks. Those from chromite-bearing rocks have both high Al and (Na + K) contents. Noteworthy is the strong tendency for the data to lie on a line of constant Al/(Na + K) ratio.

Finally fig. 7 shows the amphibole data plotted against the Mg/(Mg + Fe + Mn) atomic ratio and the number of (Na + K + Al) atoms per four chemical formula units. This plot is similar to that of ERNST (1968, fig. 10) except that (a) ferric iron has been omitted and K has been added to the ordinate, and (b) Mn has been added to the abscissa. ERNST's compilation of analyses shows a concentration exactly overlapping the range of the Fiskenæsset amphiboles. In this plot, the amphiboles from the ultramafic rocks are completely separated from those of the anorthosite-gabbro rocks on the basis of their higher Mg content. The range of (Na + K + Al) is about 3 for both groups with almost complete overlap.

Having covered the major chemical variation as a function of zonal position and rock type, the inter-chemical relations will be described.

Fig. 8 shows the relation between FeO and MnO. There is abundant evidence for a strong geochemical coherence between these elements in ferromagnesian silicates (e.g. KOSTYUK & SOBOLEV, 1969, for amphiboles). Here also the Fiskenæsset amphiboles show a strong tendency to a linear

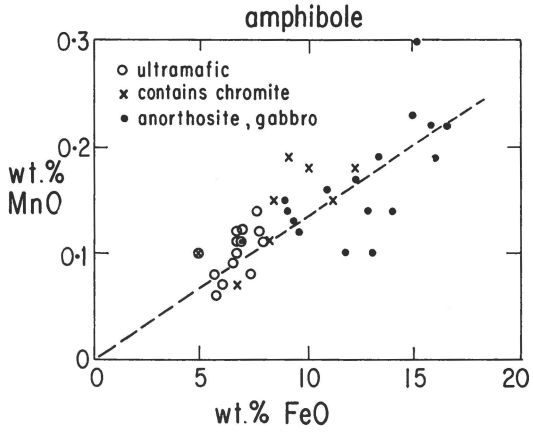

Fig. 8. The relation between wt. % MnO and FeO in the amphiboles. Each amphibole is plotted with a symbol for its host rock. The dashed line is fitted visually to pass through the origin.

coherence. Most of the data lie within two standard errors of the dashed line in fig. 8. Probably Mn is a poor element for attempting to disentangle chemical factors in the intrusion.

Fig. 9 shows the relation between TiO_2 and FeO. It is obvious that the spread of data is so large that some chemical relationship in the intrusion itself is affecting the relation between TiO_2 and FeO. In general,

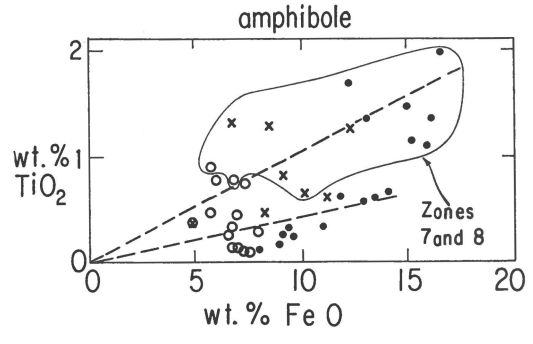

Fig. 9. The relation between wt. % TiO_2 and FeO in the amphiboles. Each amphibole is plotted with a symbol for its host rock: open circle, ultramafic; cross, chromite-bearing; dot, anorthosite or gabbro. Samples from zones 7 and 8 are enclosed by the ring. The upper dashed line was fitted visually to pass through the origin and the center of these points. The lower dashed line was fitted visually to pass through the origin and the bulk of the remaining samples.

there is a positive correlation between the two elements, as found by KOSTYUK & SOBOLEV (1969) in a general survey of calciferous amphiboles of metamorphic rocks. For the Fiskenæsset amphiboles, those from

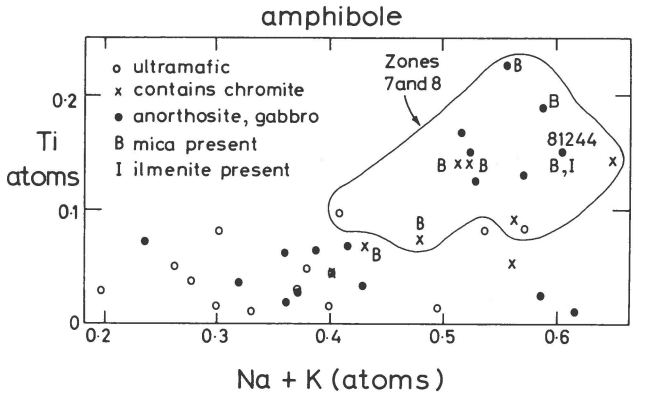

Fig. 10. The relation between the number of Ti and (Na + K) atoms per formula unit of the amphiboles. Each amphibole is plotted with a symbol for its host rock. In addition, several samples are labelled for the presence of ilmenite or mica or both (specimen 81244). Samples from zones 7 and 8 are enclosed in a ring. Note that the origin for the abscissa is not at zero.

zones 7 and 8 tend to contain more TiO_2 than those from lower zones. From the viewpoint of host-rock, there is almost a complete segregation of the amphiboles depending on whether the host-rock is ultramafic (FeO 5 to 8 wt. %, TiO_2 0 to 1 %) or anorthosite-gabbro (a curved band from FeO 8, TiO_2 0.1 to FeO 15, TiO_2 2). The amphiboles from chromite-bearing rocks occupy an area around FeO 10, TiO_2 1 (apart from the amphibole in an ultramafic rock which falls with the first group). Apparently the TiO_2–FeO distribution must be considered in terms of at least two factors: type of host rock, and the zonal position. In fig. 9 the dashed lines have no statistical significance and are merely aids for judging the distribution of data.

Fig. 10 shows the relation between Ti and (Na + K) atoms. In this plot, the major separation is between amphiboles from zones 7 and 8 with respect to those from lower zones. Seven rocks containing mica are marked with B, and these tend to come from the upper zones. One rock, 81244, contains ilmenite as well as mica but the amphibole does not have an unusual amount of TiO_2. The amphiboles from the lower zones lie in a band with TiO_2 from 0 to 0.9 atom per formula unit, and 0.2 to 0.6 atom of (Na + K) without any obvious pattern with respect to host rock type.

Fig. 11 shows the relation between NiO and MgO. The error of 0.02 in NiO must cause considerable scatter in the data. Taking this into account, it is likely that there is some coherence between Ni and Mg in these amphiboles, in accordance with data found for many ferromagnesian silicates (e.g. for olivines, SMITH, 1966; and for orthopyroxenes,

HOWIE & SMITH, 1966). However, the spread of data is sufficiently large that there may not be a 1:1 correspondence between Ni and Mg: further study with higher accuracy is desirable.

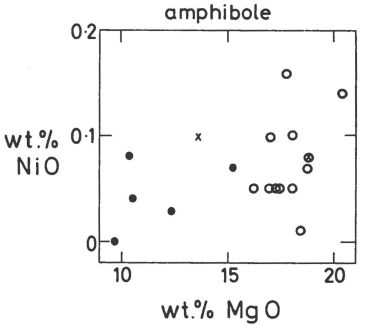

Fig. 11. The relation between wt. % NiO and MgO in those amphiboles for which NiO was measured. Each amphibole is plotted with a symbol for its host rock: open circle, ultramafic; cross, chromite-bearing; dot, anorthosite or gabbro. Note that the origin is not at zero.

Garnet. This is a rare mineral occurring only in rocks 81244 and 81235 of zone 8. FRISCH (1971) reported a garnet of similar composition, probably from zone 8. The garnet analyses of table 1a have been recalculated into atomic contents in table 1b assuming that the Fe is all ferrous or that 5 % is ferric. The latter assumption gives better summations for the X and Y sites, but increases the amount of Al assigned to the Si site. The garnet compositions are dominated by pyrope and almandine components in roughly equal amounts with minor spessartine and a small amount of Ca-bearing components, probably a mixture of andradite and grossular. Approximate compositions in end-members for the 81244 and 84428 garnets are: pyrope 46, 36; almandine 46, 50; spessartine 1, 2; andradite? 4, 4; grossular 3, 8. The Ti and Cr contents of the garnet are trivial. HOWIE & SUBRAMANIAM (1957) described the paragenesis of garnet in charnockite, enderbite and related granulites. There is a considerable range of compositions with the grossular and pyrope contents varying considerably. The Fiskenæsset garnets lie between specimens G79 and 9 in their table 3.

Olivine. All the Fiskenæsset olivines are Mg rich with a forsterite content between 74 and 86 mol % (fig. 12). The four olivines from zone 2 have 74, 76, 77 and 79 % Fo, that from zone 3 has 77, the two olivines at the zone boundary 3–4 have 82 and 86, those from zones 5 and 6 have 80 and 81, and those from zone 8 have 81 and 86 % Fo. Consequently there is a general tendency for the olivines to become more magnesian

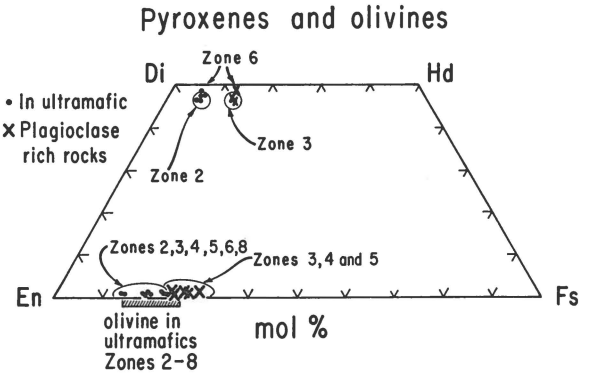

Fig. 12. Compositions of pyroxenes and olivines. The pyroxene compositions were plotted on the Di–En–Fs–Hd quadrilateral using the Ca, Mg, Fe analyses. The olivine analyses were calculated using the Mg,Fe analyses and plotted on the Fo–Fa join, here represented conventionally on the En–Fs join of the pyroxenes.

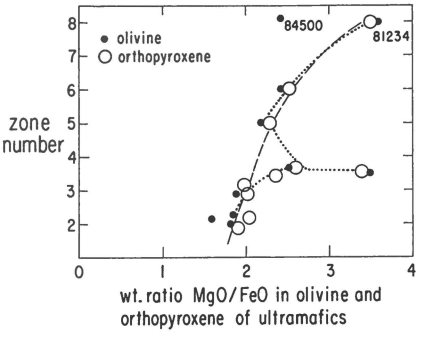

Fig. 13. Variation of wt. ratio MgO/FeO in olivine and orthopyroxene of the ultramafic rocks with zone number. The dashed line shows a simplified trend whereas the dotted line shows a complex trend with an apparent discontinuity or spike between zones 3 and 4. Rock 84500 is anomalous in several respects, as well as that implied here.

with increasing height with an apparent discontinuity near the 3–4 zone boundary (fig. 13).

Fig. 14 shows the minor elements in olivine plotted against mol % Fo and compared with the survey by SIMKIN & SMITH (1970) of terrestrial olivines from many rock types. The Mn content falls nicely within the range found by SIMKIN & SMITH (dashed lines). All but one of data points for Ni fall into the range found for terrestrial rocks, and this one for rock 84488 in zone 2 is only just off the range. There is no correlation between Ni content and zonal position.

The Ca contents of olivines from terrestrial rocks were found by SIMKIN & SMITH to divide neatly into two groups: those from extrusive

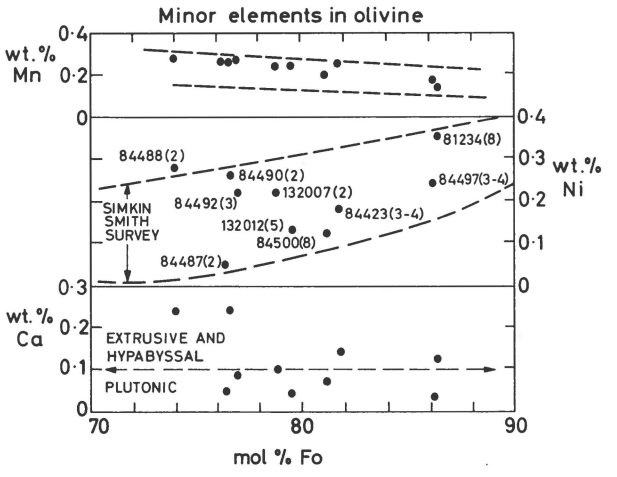

Fig. 14. The relation between the minor elements Mn, Ni and Ca on the one hand and mol % Fo on the other hand for olivines. In the upper two diagrams, the dashed lines delimit the areas in which olivines lay in the survey of SIMKIN & SMITH (1970). For the Ni analyses, each point is labelled with the number of the host rock and the zone number in brackets. For the Ca analyses, the dashed line shows the boundary found by SIMKIN & SMITH between olivines from extrusive and hypabyssal rocks (more calcic) and those from plutonic rocks (less calcic).

and hypabyssal rocks with more than 0.1 wt. % Ca, and those from plutonic rocks with less than 0.1. The Ca contents of the Fiskenæsset olivines straddle the boundary by much more than the experimental error of about 0.02 wt. %. This variation is readily interpretable in terms of partial metamorphic recrystallization of a primary igneous assemblage. Indeed the olivines with the highest Ca contents come from two rocks (84488 and 84490) showing textural evidence of a primary igneous assemblage only partly recrystallized to the polygonal texture indicative of metamorphic recrystallization (see later paper).

The electron microprobe analyses show significant amounts of Al_2O_3 (maximum 0.14) which should be significant in view of an expected detection limit near 0.03 wt. %. SIMKIN & SMITH did not find any terrestrial olivines with Al_2O_3 at the 0.02 wt. % in a quick survey, and did not make detailed studies. In lunar rocks, several studies have recorded significant amounts of Al_2O_3 in olivines. Detailed studies are needed to elucidate the factors that govern the entrance of Al into olivine. Possibly a high temperature of crystallization is an important factor. The Al could enter the olivine structure either at 2Al for $Si + (Fe^2, Mg)$ or as $Al + Fe^3$ for $Si + (Fe^2, Mg)$.

Orthopyroxene. The principal composition variation of the orthopyroxenes is shown in fig. 12. All have low calcium contents (maximum 1.5

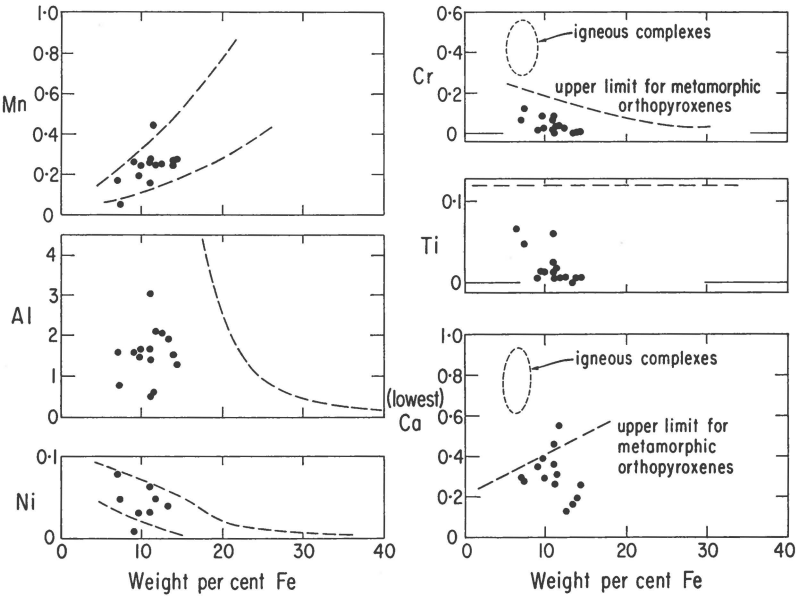

Fig. 15. The relation between the minor elements Mn, Al, Ni, Cr, Ti and Ca on the one hand and wt. % Fe on the other hand for orthopyroxenes. The dashed lines refer to data obtained by Howie & Smith (1966) for orthopyroxenes primarily from high-grade metamorphic rocks. For Mn and Ni the dashed lines show the limits found by Howie & Smith. For Al and Ti, the dashed line shows the upper limits. For Cr and Ca the range of data for a few orthopyroxenes from igneous complexes is shown: it should be noted that Howie & Smith deliberately plotted the lowest amount of Ca recorded in electron microprobe analyses in order to minimize the effect of augite lamellae.

mol % Wo) and plot near to the En–Fs join. Orthopyroxenes from the ultramafic rocks are more magnesian (77 to 86 mol % En) than those from plagioclase-rich rocks (70 to 76 mol % En).

Fig. 13 shows that the variation with zonal position of the MgO/FeO ratio of the orthopyroxenes is closely similar to that of the olivines. There is a general tendency for the orthopyroxenes to become more magnesian upwards, but with a major jump to more Mg-rich compositions at the 3–4 zone boundary.

Fig. 15 shows the minor elements compared with data obtained by Howie & Smith (1966) mostly for metamorphic orthopyroxenes. Within experimental error, the Mn contents fall within the range found by Howie & Smith, presumably reflecting the strong coherence between Fe and Mn in all ferromagnesian silicates.

The Ca contents are low and lie in the range found for metamorphic orthopyroxenes (fig. 15); they are lower than those found in orthopyroxenes from igneous complexes such as the Bushveld. For the latter igneous

specimens the lowest Ca readings were used by HOWIE & SMITH in order to avoid exsolved lamellae of augite. Probably the low Ca contents of the Fiskenæsset orthopyroxenes indicate temperatures considerably below 1000° C, but definite values cannot be established without further work.

The Fiskenæsset orthopyroxenes have a maximum Al content af about 3 wt. %, well below the maximum value found by HOWIE & SMITH for metamorphic orthopyroxenes with this range of Fe contents. The entrance of Al into orthopyroxene is favoured by both pressure and temperature (BOYD & ENGLAND, 1964; BOYD, 1970), but the actual amount depends on the bulk composition of the rock and the minerals coexisting with the orthopyroxene. It is not possible to use the Al contents of the Fiskenæsset orthopyroxenes to determine crystallization conditions, but the combination of low Ca content and modest Al contents are consistent with moderate temperatures and pressures.

The orthopyroxene from rock 84488 has anomalously low Al and fairly high Ca compared to the majority of the orthopyroxene. It is this rock that has an igneous texture and an olivine with high Ca content. Tentatively, we suggest that metamorphic recrystallization of the orthopyroxenes results in reduction of the Ca content and increase in the Al content, perhaps a result of lowered temperature and heightened pressure (see later paper).

The Ni and Cr contents fall within the limits found by HOWIE & SMITH for metamorphic orthopyroxenes. The Ti contents are low, mostly near the detection level of 0.02 wt. %.

Clinopyroxene: diopside and sahlite. Fig. 12 shows the positions of the clinopyroxenes on the Di–Hd–En–Fs quadrilateral. All the samples are in or close to the diopside field. Those from the ultramafic rocks cluster near the composition $Wo_{47}En_{46}Fs_7$ and are technically diopsides, while those from the plagioclase-rich rocks cluster near the composition Wo_{47} $En_{39}Fs_{14}$ and are technically sahlites. The two samples from zone 6 are richer in Wo molecule than the samples from zones 2 and 3, but the difference may be in the range of experimental error. From fig. 12, it may be seen that the orthopyroxenes show exactly the same correlation of Fs content with rock type, with the higher Fs content deriving from the orthopyroxenes from the plagioclase-rich rocks.

Looking at the minor elements (table 4a), it can be seen that the diopsides contain more Ti, less Al and less Na than for the sahlites. The higher content of Al and Na in the sahlites may result from coexistence with plagioclase. Looking back at the orthopyroxenes, there is a similar tendency for Ti and Al whereas the Na content is too near the detection level for a comparison to be valid. The Mn contents of the sahlites (0.18

to 0.22) lie in the middle of the range for the diopsides (0.14 to 0.29), showing no correlation with the iron content.

The obvious conclusion for both the orthopyroxenes and the clinopyroxenes is that the major and minor elements of both show distinct patterns related to the type of host rock.

Yet again, rock 84488 is anomalous: its clinopyroxene has a much lower Wo content than all the other clinopyroxene, consistent with igneous crystallization without metamorphic recrystallization.

Mica. All the micas can be classified as phlogopite. They are restricted to zones 7 and 8, except for a minor occurrence in rock 132008 at the boundary between zones 3 and 4. Out of the eight rocks containing phlogopite, five also carry chromite. All the micas from these chromite-bearing rocks contain a substantial amount of chromium (0.8 to 1.2 wt. % Cr Cr_2O_3) whereas those from the chromite-free rocks contain little chromium.

The analyses of table 6a assume that all the iron is in the divalent state and the titanium in the quadrivalent state. The calculated atomic contents of table 6b also assume these valence states, and could change significantly if a considerable part of the Fe and Ti is in the trivalent state. The analyses in table 6b show values of 1.76 to 1.85 for the large cation site and 5.78 to 5.91 for the intermediate cation site, which values are lower than the ideal values for a trioctahedral mica. The calculated values would be raised somewhat by transfer of Fe from the divalent to trivalent state and reduced by transfer of Ti from the quadrivalent to trivalent state. Probably the actual changes would not be sufficient to change the cation totals markedly, and it is essentially certain that the Fiskenæsset phlogopites contain some dioctahedral constituents.

The strict join phlogopite to annite requires the composition $K(Mg, Fe^2)_3\ AlSi_3O_{10}(OH)_2$. The Fiskenæsset phlogopites contain too many Al atoms (1.4 to 1.6 per 12 oxygen atoms) to fit this join. Since the number of Si atoms (2.7 to 2.8 per 12 oxygen atoms) is lower than 3, it is necessary to incorporate some end-member such as eastonite and siderophyllite.

The deficiency of (Na + K + Ca) atoms in the *X* site (about 0.9 instead of 1 per 12 oxygen atoms) suggests either vacancies or substitution of some oxygen-hydrogen samples such as water or $(H_3O)^+$. No microprobe analyses have been made so far for fluorine. Obviously some classical analyses of mica are desirable together with spectral studies in order to clarify problems of the chemical composition and oxidation state of iron and titanium.

The small but definite contents of NiO, CaO and Na_2O are worthy of mention since these do not suffer from contamination as in many old classical analyses. The MnO contents are rather low indicating that mica

tends not to accept this element. The TiO_2 contents are fairly high but well below the amounts found in the Mg-rich phlogopites from a variety of rock types (e.g. DAWSON *et al.*, 1970).

Plagioclase. Fig. 16 shows the trend of An content with zonal position. The remarkable feature is the distinct increase of An content for rocks containing chromite compared with the An content for neighbouring plagioclase from chromite-free rocks.

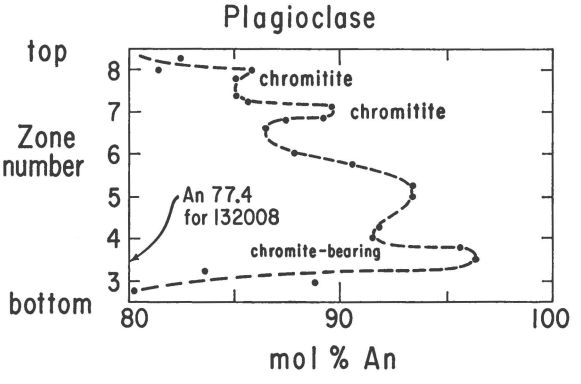

Fig. 16. The variation of An content of plagioclase with zone number. The dashed line was drawn by eye. Sample 132008 has a lower An content than the other samples.

The plagioclase is remarkably calcic with most samples lying in the range An_{80} to An_{96}. One specimen (132008) is anomalous with respect to its neighbours having a plagioclase with composition An 77.4 rather than an expected value near 90. This is not surprising because the plagioclase consists of both zoned megacrysts and zoned granules associated with phlogopite plates penetrating both plagioclase and amphibole. Detailed study of the range of An content is needed. The leuco-gabbros especially of zone 5 have plagioclase megacrysts, some of which show normal zoning with sodic margins down to about An_{60}, but the centers of the grains appear primary. The plagioclases in most of the rocks studied have a polygonal fabric of equigranular grains and show little or no evidence of metasomatism.

Detailed microprobe analyses of plagioclase, together with comprehensive *X*-ray analyses are planned. Preliminary studies show that the minor element content of the plagioclase is low (perhaps partly because of exsolution of beautiful needles of amphibole (?)), indicating equilibration to a low temperature.

Spinel (*pleonaste*). The six analyses of green spinel are arranged in order of decreasing Cr content in table 8a. There is a severe problem with the

electron microprobe analyses since the oxidation state of the iron is not known. The atomic contents of table 8b were calculated to give the closest fit of the sums of the octahedral and tetrahedral cations to 16 and 8 respectively, requiring that about one-third to one-sixth of the iron is in the ferric state. However, these estimates are highly uncertain, and require checking by better microprobe analyses and gravimetric analyses of iron.

The chromium content bears no relation to zonal position because zone 8 contains a spinel with the lowest Cr content and also a spinel with nearly the highest.

The simplest term for the spinels is pleonaste with the modifier chromian for those rich in Cr. The major part of the composition can be expressed by the join between true spinel $MgAl_2O_4$ and hercynite $FeAl_2O_4$, but the extent of minor element substitution is too complex to allow detailed assignment into end-members.

The SiO_2 content ranges from 0.1 to 0.9 wt. %. The TiO_2 content is almost zero, with the highest value only 0.07 %. Coexisting amphiboles contain considerable titanium, leaving the obvious conclusion that the Fiskenæsset pleonastes discriminate strongly against Ti. The NiO content is higher than the MnO content in all the pleonastes averaging about 0.4 wt. % compared to 0.2 wt. %. The CaO content is significant, varying from 0.05 to 0.22 wt. %.

The compositions show an obvious resemblance to those of the red spinels from some Apollo 14 rocks from the Moon (e.g. STEELE, 1972) with overlap of ranges for most of the elements. The lunar spinels contain more Ti (possibly trivalent?).

Chromite. The second type of Fiskenæsset spinel mineral, viz. chromite, has compositions shown in tables 9a and b. Again there are no direct data on the oxidation state of iron, and the partitioning in table 9b was made to equalize the deviation of the X and Y cations from stoichiometry. The chromite analyses were poorly calibrated, and a detailed study will be reported shortly. X-ray fluorescence and optical spectrographic analyses of Fiskenæsset chromites were reported by GHISLER & WINDLEY (1967) together with detailed information on the occurrence.

Magnetite. The third type of Fiskenæsset spinel mineral, viz. magnetite, has compositions shown in table 10. The zonal variation of composition is shown in fig. 17. Magnetite occurs most abundantly in zones 2 and 3 with lesser amounts in zones 6 and 8. Fig. 17 shows a well-defined reduction with height in zones 2 and 3 of the contents of MgO, TiO_2, Al_2O_3 and Cr_2O_3. Sample 84484 in zone 6 comes from a very thin layer, and has higher amounts of these elements than the magnetite from zone 3–4.

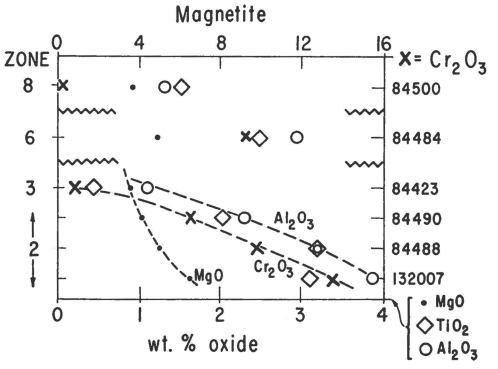

Fig. 17. The variation of minor oxides MgO, TiO_2, Al_2O_3 and major oxide Cr_2O_3 in magnetite as a function of zonal position. The number of the host rock is given at the right. The scale for Cr_2O_3 is given at the top, and that for MgO, TiO_2 and Al_2O_3 at the bottom. The dashed lines were fitted by eye to represent trends in zones 2 and 3 for MgO, Cr_2O_3 and Al_2O_3.

The rock 84500 probably comes from an ultrabasic rock associated with the overlying meta-volcanic amphibolite. All the magnetites contain significant amounts of SiO_2 and CaO, in the range as for the analyses listed in DEER *et al.* (1963). Fig. 18 shows that there is a strong correlation between Cr_2O_3 on the one hand and MgO, Al_2O_3, TiO_2, SiO_2, MnO, NiO and CaO irrespective of zonal position. More detailed data on magnetite will be given in a later paper.

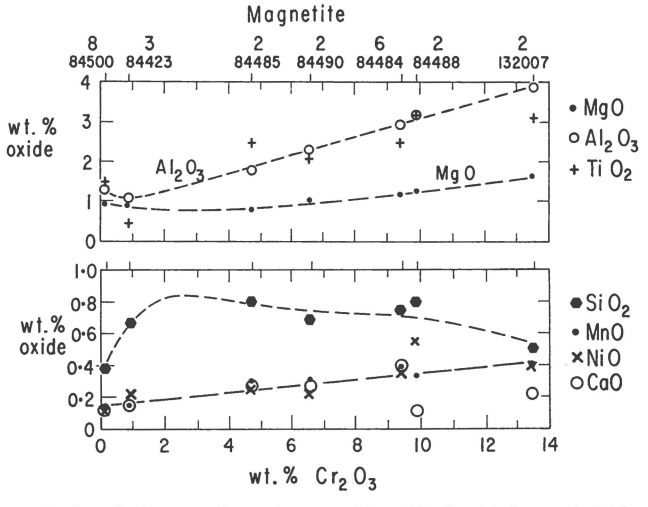

Fig. 18. The relation between the minor oxides MgO, Al_2O_3 and TiO_2 (upper diagram) and SiO_2, MnO, NiO and CaO (lower diagram) with respect to the major oxide Cr_2O_3 in magnetites. The numbers of the host rock and the zone are given at the top. The dashed lines were fitted by eye.

Ilmenite. The fourth opaque mineral is ilmenite, found only in rock 81244. A complete analysis was not made, but the following minor elements were found: Al_2O_3 0.0, Cr_2O_3 0.10, MnO 0.17, MgO 1.2, NiO 0.01, CaO 0.02 wt. %. Full details of ilmenites will be given in a later paper.

CHEMICAL DISTRIBUTION BETWEEN COEXISTING MINERALS

In this section, some inter-element distributions between coexisting minerals will be considered. Potentially these distributions may permit estimates of the degree of equilibration, and in favourable circumstances might act as thermometers or barometers. However, there are many problems as emphasized, for example, by KRETZ (1960). Particularly of interest are any distributions which reflect an original igneous assemblage. The present description concerns minerals mostly occurring in rocks with textures indicating metamorphic recrystallization. A later paper concentrates on the rare rocks, including 84488, with indications of a relict igneous texture only partly recrystallized. To anticipate the conclusion for the sake of clarity, the inter-element distributions suggest only partial equilibration. The original element distribution is interpreted as resulting from crystallization from a liquid with extensive gravity differentiation to give a strongly layered assemblage. Subsequent metamorphism led to recrystallization of some but not all minerals with chemical migrations over only small distances mostly less than the width of the layers.

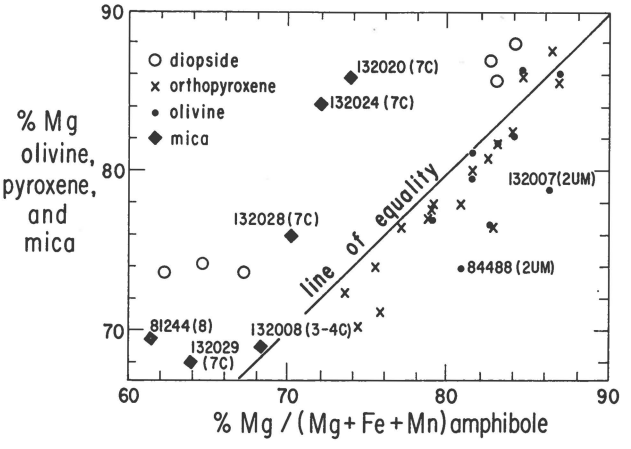

Fig. 19. Relation between atomic per cent Mg/(Mg + Fe + Mn) for olivine, pyroxene and mica with respect to coexisting amphibole. Certain samples have been labelled with the rock type.

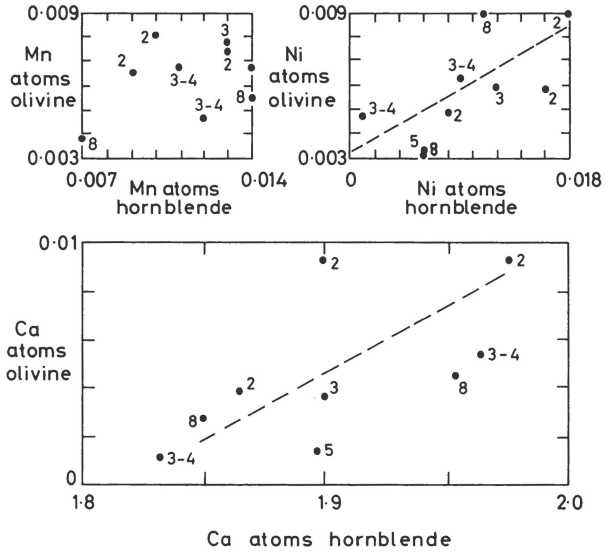

Fig. 20. Distribution of Mn, Ni and Ca atoms between coexisting olivine and hornblende. The number of atoms was calculated with respect to 4 atoms of oxygen for olivine and 23 for the water-free amphibole. The samples are labelled with the zone number. The dashed lines were fitted by eye. Note that some of the scales do not begin at zero.

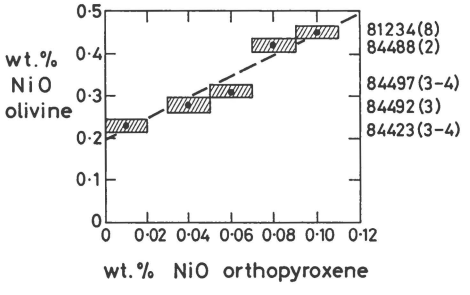

Fig. 21. Distribution of wt. % NiO between coexisting olivine and orthopyroxene. The rectangles show plus and minus one standard deviation. The dashed line was fitted by eye. At the right are the rock and zone numbers.

The net effect of these sequential processes is to give a very confusing set of distributions. Theoretically one can envisage the lateral range of equilibration decreasing with temperature as the diffusion distance falls so that equilibration at a higher temperature may occur over distances greater than the grain size while that at lower temperature will occur only inside individual grains. The present data are concerned with

chemical distributions on the scale of the grain size, and give no information on a scale below a micrometer such as could occur for exsolution on a unit-cell scale.

Ferromagnesian minerals. Fig. 19 shows the Mg/Fe distribution between coexisting ferromagnesian minerals. The order of preference of magnesium is mica and diopside over hornblende with olivine and ortho-

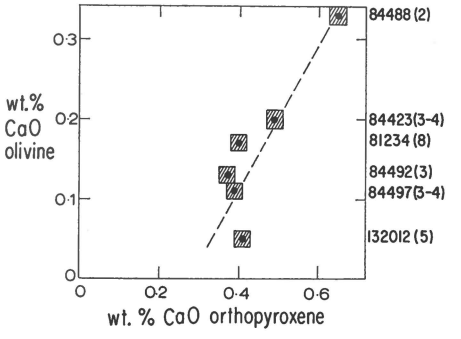

Fig. 22. Distribution of wt. % CaO between coexisting olivine and orthopyroxene. The rectangles show plus and minus one standard deviation. The dashed line was fitted by eye. At the right are the rock and zone numbers.

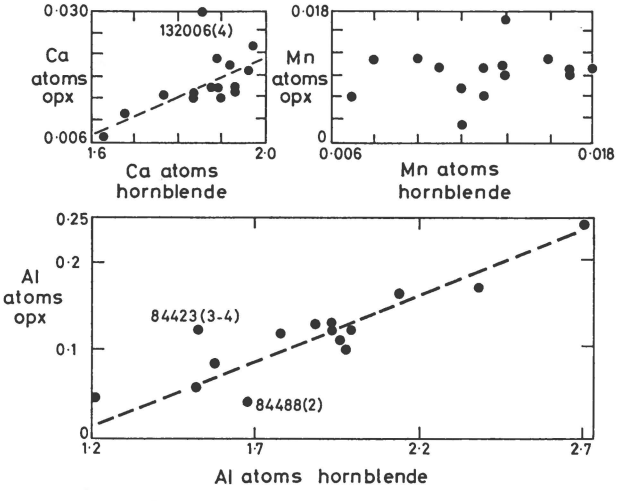

Fig. 23. Distribution of Ca, Mn and Al atoms between coexisting orthopyroxene and hornblende. The number of atoms was calculated with respect to 6 atoms of oxygen for orthopyroxene and 23 for the water-free amphibole. Several unusual samples are labelled with the rock and zone numbers. The dashed lines were fitted by eye.

pyroxene the least favoured. Three samples with coexisting diopside and orthopyroxene allow a temperature estimate using the method of KRETZ (1963):

	Mg/Fe (opx)	Mg/Fe (cpx)	K_D
84484	4.54	7.60	0.60
84485	3.38	6.21	0.54
84488	3.59	3.49	1.03

The distribution coefficient for the first two sets falls in the range for metamorphic assemblages whereas the third one fits with igneous samples. This is consistent with the textural evidence for these samples. Fig. 20 shows the distribution of Mn, Ni and Ca between olivine and hornblende. The Mn distribution is erratic, but the Ni and Ca distributions show weak correlations.

Figs 21 and 22 show the distribution of NiO and CaO between coexisting olivine and orthopyroxene. Within experimental error, most of the data are consistent with linear trends which do not pass through the origin.

Fig. 23 shows the distribution of Ca, Mn and Al between coexisting orthopyroxene and hornblende. There are fairly good positive correlations for Ca and Al but the Mn distribution shows no obvious trend.

Fig. 24 shows the distribution of Ti, Na, Mn and Al between clinopyroxene and hornblende. No obvious correlations occur.

Fig. 25 shows the distribution of K between amphibole and mica. For the samples from zones 7 and 8 there is a good positive correlation, but the point for rock 132008 in zone 3–4 falls off the trend.

Hornblende and plagioclase. Figs 26 and 27 show the distribution of Al and Na between hornblende and plagioclase using various items for convenience. The Al distribution is erratic but there may be a weak positive correlation. The Na distribution shows a fairly good negative correlation with only two deviant samples. This negative correlation is remarkable. It is possible that it reflects incomplete chemical migration during metamorphic equilibration between amphibole and plagioclase? Pertinent to this is the observation that zoned plagioclase appears to occur only in the neighbourhood of amphibole grains. A detailed study is planned to investigate whether this preliminary observation applies throughout the Fiskenæsset rocks.

Fig. 28 shows that there is a moderate positive correlation between the Na content of the plagioclase and the K content of the hornblende. The presence of mica seems to have no effect on the correlations.

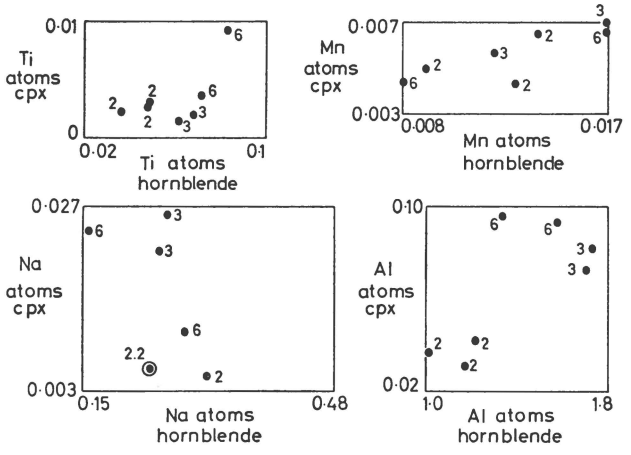

Fig. 24. Relation between Ti, Mn, Na and Al atoms of coexisting clinopyroxene and hornblende. The number of atoms was calculated with respect to 6 atoms of oxygen in the pyroxene and 23 atoms for water-free amphibole. The samples are labelled with the zone number. Note that all but one of the scales do not start at zero.

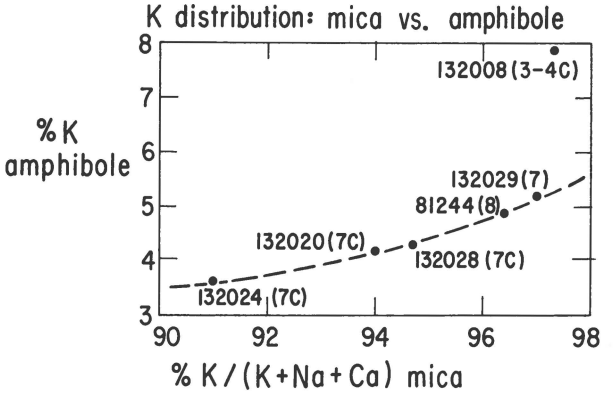

Fig. 25. Distribution of K between coexisting phlogopite and amphibole expressed as the atomic ratio K/(K + Na + Ca). The samples are labelled with the rock and zone number: four samples are from chromite-bearing rocks denoted C. The dashed line was fitted by eye for the five lower points.

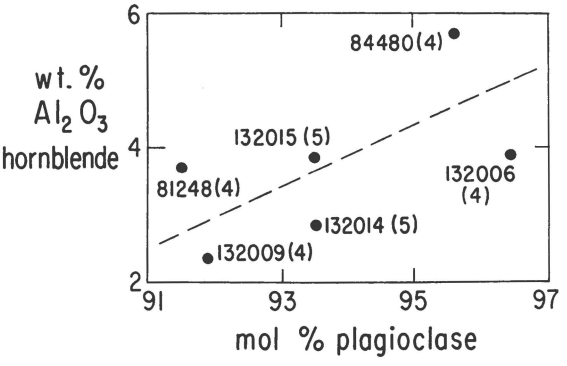

Fig. 26. Distribution of Al between coexisting hornblende and plagioclase using wt. % Al_2O_3 for the former and mol % An for the latter. The samples are labelled with the rock and zone number. The dashed line was inserted by eye.

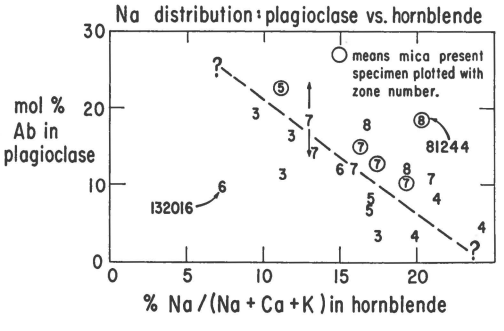

Fig. 27. Distribution of Na between coexisting hornblende and plagioclase, the former expressed as atomic ratio Na/(Na + Ca + K) and the latter as mol % Ab. Each sample is plotted with its zone number while two unusual ones are labelled with the rock number as well. Presence of mica is shown by a circle around the zone number. The dashed line was fitted by eye. The plagioclase in a sample from zone 7 is chemically zoned as indicated qualitatively with the two arrows.

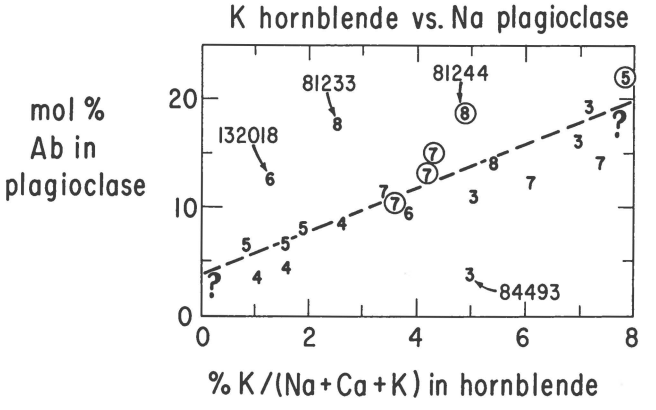

Fig. 28 The relation between potassium content of hornblende (as expressed by the atomic ratio K/(Na + Ca + K)) and the sodium content of the coexisting plagioclase (as expressed by mol % Ab). Each sample is plotted with its zone number. The circle shows the presence of mica. Four unusual samples are labelled with the rock number. The dashed line was fitted by eye.

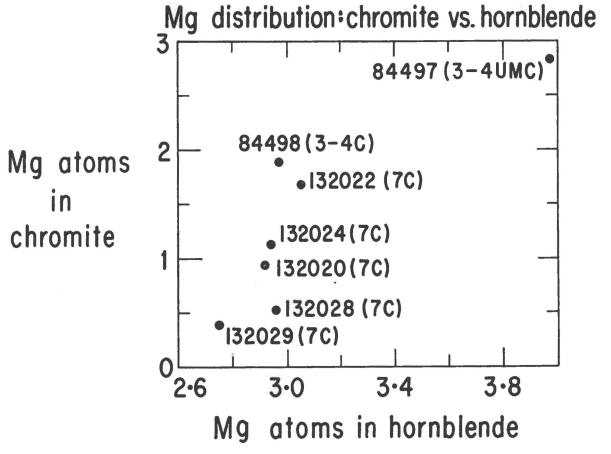

Fig. 29. The distribution of Mg between coexisting chromite and hornblende. The number of Mg atoms was calculated with respect to 32 oxygens in chromite and 23 oxygens in water-free hornblende. Each sample is labelled with the rock and zone numbers. The symbols UM and C stand for ultramafic rock and presence of chromite.

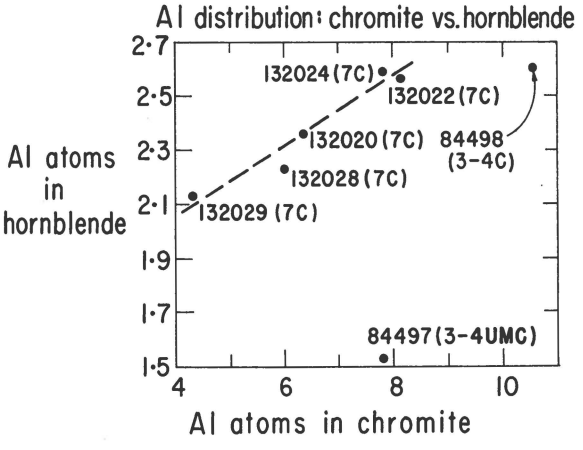

Fig. 30. The distribution of Al between coexisting chromite and hornblende. The number of Al atoms was calculated with respect to 32 oxygens in chromite and 23 oxygens in water-free hornblende. Each sample is labelled with the rock and zone numbers. The symbols UM and C stand for ultramafic rock and presence of chromite. The dashed line was fitted by eye for the chromites from zone 7.

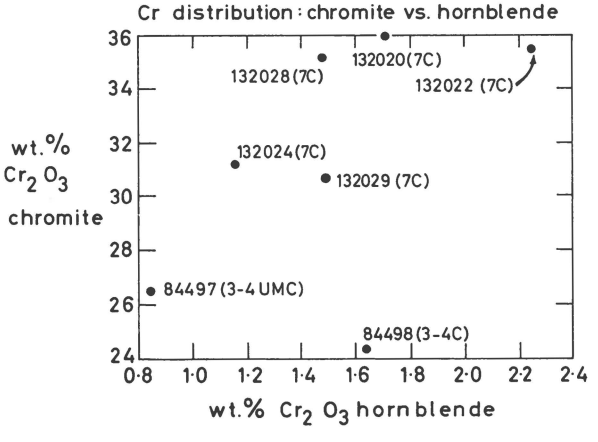

Fig. 31. The distribution of wt. % Cr_2O_3 between coexisting chromite and hornblende. Each sample is labelled with the rock and zone number. The symbols UM and C stand for ultramafic rock and presence of chromite. Note that the scales do not start at zero.

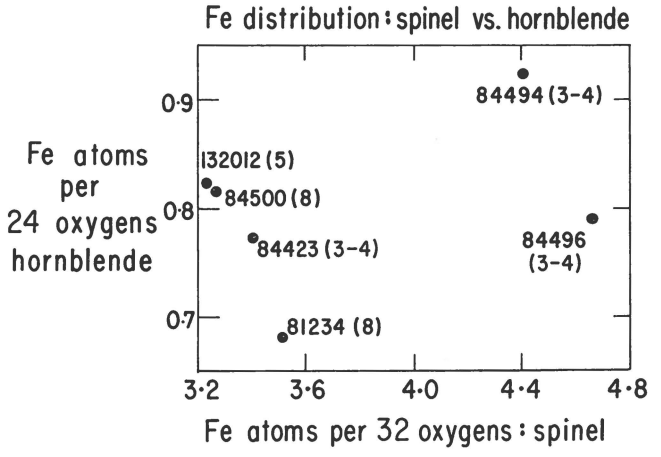

Fig. 32. The distribution of Fe atoms between hornblende and spinel. The samples are labelled with the rock and zone numbers. Note that the scales do not begin at zero. The number of Fe atoms in hornblende was calculated for 23 oxygens in water-free amphibole.

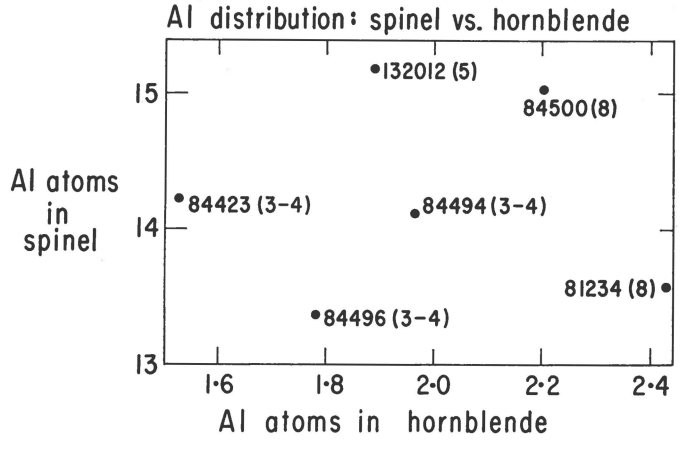

Fig. 33. The distribution of Al atoms between hornblende and spinel. The number of Al atoms was calculated with respect to 23 oxygen atoms in water-free hornblende and 32 oxygens in the spinel. The samples are labelled with the rock and zone numbers.

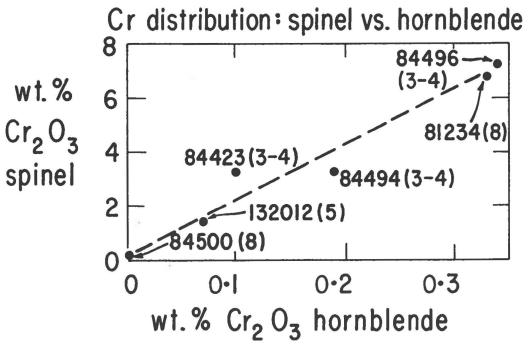

Fig. 34. The distribution of Cr_2O_3 between hornblende and spinel. The samples are labelled with the rock and zone numbers. The dashed line was fitted by eye to pass through the origin.

Spinels and hornblende. Figs 29, 30 and 31 show the distribution of Mg, Al and Cr between chromite and hornblende. The distribution of Cr is erratic, but the distribution of Mg and Al show moderate positive correlations.

Figs 32, 33 and 34 show the distribution of Fe, Al and Cr between spinel and hornblende. The distributions of Fe and Al are random, but there is a good positive correlation for Cr.

CONCLUSIONS

The main conclusion from this study is that the mineral chemistry is interpretable in terms of a primary igneous crystallization with cryptic chemical variations only partly reorganized by subsequent metamorphic re-equilibration. This refers in particular to magnetite, olivine, orthopyroxene, plagioclase and hornblende. As it was concluded in part I (WINDLEY *et al.*, 1973) that the differentiation trend of the Fiskenæsset intrusion is still preserved, that there was appreciable water in the magma, and therefore that amphibole was a primary igneous phase, it was expected that some minerals including amphibole might retain igneous cryptic chemical trends.

The Mg/Fe ratio of the bulk rocks and individual minerals appears to have been particularly insensitive to change during recrystallization and so proves to be one of the most useful indicators of the igneous fractionation pattern. With height in the intrusion it decreases in the bulk rocks, increases in olivine and orthopyroxene, and first increases and then decreases in amphibole; noticeably clinopyroxene shows no

systematic trend. The upward increase in alkalis in the bulk rocks is reflected by a similar increase in the Ab content of plagioclase, and by the appearance of phlogopite in upper zones. In spite of the fact that garnet occurs in zone 8 (anorthosites with An_{80} plagioclases), it has low calcium and high pyrope and almandine components; this correlates with the observation in some sections that it has nucleated on spinel.

Amphiboles vary in composition from magnesio-hornblende through tschermakitic hornblende to tschermakite, individual zones of the intrusion having amphiboles with a particular range in composition. Clinopyroxene in ultramafic rocks is near diopside $Wo_{47}En_{46}Fs_7$ and in gabbroic and anorthositic rocks it is near sahlite $Wo_{47}En_{39}Fs_{14}$. Olivine and orthopyroxene are Mg-rich, lying in the range 74–86 mol % forsterite and 70–86 mol % enstatite respectively, and plagioclase varies from An_{96} to An_{80}. The zone 3–4 boundary is an important chemical position in the intrusion as it marks a significant jump in the Mg/Fe ratio of olivine and orthopyroxene and a major peak at An_{96} in the plagioclase curve. The An content of plagioclase increases markedly in the presence of chromite, probably due to the fact that plagioclase precipitated as a cumulus phase in chromite-bearing layers whereas it was a fractionate or intercumulus phase in the chromite-free layer of zone 7 and in zones 6 and 8.

Redistribution of elements within and amongst grains during the metamorphism appears to have been small. Coexisting ferromagnesian minerals have attained, or retained, a degree of equilibrium as indicated by good positive correlations of:

Mg (hornblende-olivine, orthopyroxene and clinopyroxene)
Ca, Ni (hornblende-olivine) and (orthopyroxene-olivine)
Al, Ca (hornblende-orthopyroxene)
Mn (hornblende-clinopyroxene)
K (hornblende-phlogopite)

Some elements, on the other hand, show erratic partitioning:

Mn (hornblende-olivine) and (hornblende-orthopyroxene)
Na, Al Ti (hornblende-clinopyroxene)

There is an interesting strong negative correlation between Na in plagioclase and hornblende suggesting migration and interchange of sodium during recrystallization, whereas K in hornblende has a positive correlation with Na in plagioclase. There is moderate partitioning of Mg and Al between chromite and hornblende, and of Cr between spinel and hornblende, but erratic distribution of Fe and Al between spinel and hornblende. Viewed as a whole the present chemical state of the minerals

in the intrusion is one of disequilibrium as they have a mixture of both igneous and metamorphic characteristics.

We consider it premature at this stage to work out detailed metamorphic distribution coefficients until more is known about K_D values from primary phases. Some leuco-gabbros retain their igneous plagioclase megacrysts and rare ultramafic rocks, such as 84488, retain their igneous olivine, orthopyroxene, clinopyroxene, hornblende crystals and opaque oxides. These ferromagnesian primocrysts are remarkable poikilitic megacrysts up to 1 cm across that are sieved with ore dust and show little evidence of metamorphic recrystallization. They are to be the subject of a special study on the chemistry of the igneous minerals of the intrusion. Remnants of similar but smaller ore-filled grains occur in other ultramafic layers of zone 2.

Further petrographic conclusions will be made when a special study of the chemistry of the opaque oxides is published. Also whole rock analyses are currently being made of the same samples used for this study.

The aim of this paper has been to produce a general picture of the chemical state of the minerals in the Fiskenæsset intrusion. We think that it is necessary to have a broad initial survey before embarking on detailed studies of specific aspects of mineralogy or petrology on this complex group of rocks. Clearly the Fiskenæsset intrusion offers scope for innumerable studies on an array of mineralogical, chemical and petrological problems. It is now possible to see where some of the more fruitful paths lie for future research. For example, some minerals have interesting and unusual compositions, viz. tschermakitic hornblende and chromic tschermakite, which warrant more detailed mineralogy, some elements and minerals are better than others for studying inherited igneous chemical patterns, and some coexisting mineral pairs will give better metamorphic distribution coefficients than others. It may be possible in future years to work out a detailed movement pattern for elements within and amongst grains during metamorphic recrystallisation of this layered igneous intrusion.

Acknowledgements

We thank the National Science Foundation for grant GA 21123, and Mrs. I. BALTUSKA, P. S. MATKOVITS, O. DRAUGHN and R. ZECHMAN for technical help. R. K. HERD kindly suggested improvements to the manuscript. We thank the director of The Geological Survey of Greenland for permission to publish these results.

TABLES

Table 1a. *Garnet: reconnaissance microprobe analyses*

GGU No.	81244	84428
Zone	8	8
SiO_2	39.1	40.1
TiO_2	0.02	0.01
Al_2O_3	21.7	22.6
Cr_2O_3	0.04	0.00
FeO	24.9	23.4
MnO	0.78	0.51
MgO	9.48	12.63
NiO	nd	nd
CaO	4.26	2.31
Na_2O	nd	nd
K_2O	nd	nd
	100.2	101.5

nd not detected.

Table 1b. *Garnet: atomic contents for 24 oxygens*

GGU No.	81244*	84428*		81244**	84428**
Zone	8	8		8	8
Si	5.984	5.960	Si	5.964	5.942
Al	0.016	0.040	Al	0.036	0.058
Al	3.898	3.919	Al	3.865	3.867
Ti	0.002	0.001	Ti	0.002	0.001
Cr	0.005	0.0	Cr	0.005	0.0
Mg	2.163	2.798	Fe^3	0.159	0.145
Fe	3.186	2.908	Fe^2	3.018	2.754
Mn	0.101	0.064	Mg	2.157	2.789
Ca	0.699	0.368	Mn	0.101	0.064
			Ca	0.697	0.367
ΣX	6.149	6.138			
ΣY	3.905	3.920	ΣX	5.973	5.974
			ΣY	4.031	4.012

* Assuming Fe is ferrous.
** Assuming 5 % Fe is ferric.

Table 2a. *Olivine: reconnaissance microprobe analyses*

GGU No.	132007	84487	84488*	84490*	84492*	84497*
Zone	2 UM	2 UM	2 UM	2 UM	3 UM	3–4 UMC
SiO_2.....	37.9	38.9	37.0	39.2	37.5	39.4
TiO_2.....	0.02	0.00	0.01	0.01	0.00	0.0
Al_2O_3.....	0.01	0.02	0.08	0.00	0.14	0.04
Cr_2O_3.....	0.00	0.00	0.01	0.00	0.00	0.03
FeO.....	19.8	21.6	23.6	21.5	21.1	13.0
MnO	0.30	0.34	0.36	0.34	0.35	0.22
MgO.....	41.6	39.1	37.5	39.7	39.6	45.3
NiO	0.28	0.06	0.42	0.24	0.28	0.31
CaO.....	0.14	0.07	0.33	0.34	0.13	0.04
	100.1	100.0	99.1	101.4	99.4	98.5

GGU No.	132012	84500	81234	84423*	84484*
Zone	5 UM	8 UM	8 UM	3–4 UM	6 UM
SiO_2.....	38.3	39.1	40.1	39.2	39.3
TiO_2.....	0.01	0.01	0.01	0.02	nd
Al_2O_3.....	0.03	0.07	0.11	0.04	nd
Cr_2O_3.....	0.00	0.01	0.02	0.00	nd
FeO.....	18.7	17.6	13.0	17.3	17.4
MnO	0.31	0.26	0.18	0.32	nd
MgO.....	40.9	42.7	46.6	43.7	42.3
NiO	0.16	0.15	0.45	0.23	nd
CaO.....	0.05	0.10	0.17	0.20	nd
	98.5	99.9	100.5	101.0	99.0

* Major elements reduced by 1.5 %.
nd not detected.

Note added in proof.

The total and the individual oxides of the analyses were rounded separately, and therefore the rounded total is slightly different from the total of the individual rounded oxides.

Table 2b. *Olivine: atomic contents for 4 oxygens*

GGU No.	132007	84487	84488	84490	84492	84497
Zone	2 UM	2 UM	2 UM	2 UM	3 UM	3–4 UMC
Si	0.978	1.007	0.981	1.002	0.983	0.999
Al	0.0003	0.0006	0.0025	0.0	0.004	0.0012
Ti	0.0004	0.0	0.0002	0.0002	0.0	0.0
Cr	0.0	0.0	0.0002	0.0	0.0	0.0006
Mg	1.600	1.508	1.483	1.513	1.547	1.712
Ni	0.0058	0.0012	0.0090	0.0049	0.0059	0.0063
Fe	0.427	0.467	0.523	0.460	0.462	0.275
Mn	0.0066	0.0075	0.0081	0.0074	0.0078	0.0047
Ca	0.0039	0.0019	0.0094	0.0093	0.0037	0.0011
ΣM	2.004	1.986	2.035	1.995	2.031	2.001
% Mg	78.9	76.4	74.0	76.7	77.0	86.2

GGU No.	132012	84500	81234	84423	84484
Zone	5 UM	8 UM	8 UM	3–4 UM	6 UM
Si	0.997	0.995	0.993	0.988	1.006
Al	0.0009	0.002	0.0032	0.0012	nd
Ti	0.0002	0.0002	0.0002	0.0004	nd
Cr	0.0	0.0002	0.0004	0.0	nd
Mg	1.586	1.620	1.720	1.641	1.615
Ni	0.0033	0.0031	0.009	0.0047	nd
Fe	0.407	0.374	0.269	0.364	0.372
Mn	0.0068	0.0056	0.0038	0.0068	nd
Ca	0.0014	0.0027	0.0045	0.0054	nd
ΣM	2.005	2.008	2.009	2.023	1.987
% Mg	79.6	81.2	86.4	81.8	81.3

nd not detected.

Table 3a. *Orthopyroxene: reconnaissance microprobe analyses*

GGU No. .	132006	84485	84488*	84492*	84494*	84496*	84497*	132009
Zone	4	2 UM	2 UM	3 UM	3 UM	3–4 UM	3–4 UMC	4
SiO_2.....	51.7	55.1	54.4	53.2	52.8	53.8	55.8	53.3
TiO_2.....	0.01	0.03	0.10	0.04	0.02	0.02	0.08	0.01
Al_2O_3.....	3.88	1.12	0.93	3.11	2.61	2.78	1.44	2.34
Cr_2O_3.....	0.05	0.05	0.12	0.01	0.10	0.12	0.17	0.01
FeO	15.2	14.8	14.3	14.3	14.4	12.5	9.58	18.6
MnO	0.31	0.57	0.35	0.34	0.33	0.25	0.06	0.35
MgO.....	28.0	28.1	28.9	28.9	28.6	29.9	32.3	25.1
NiO	0.06	nd	0.08	0.04	0.04	0.04	0.06	nd
CaO	0.77	0.43	0.65	0.37	0.51	0.55	0.39	0.37
Na_2O	0.03	0.00	0.01	0.02	0.02	0.02	0.01	0.00
K_2O	0.00	0.02	0.02	0.01	0.01	0.01	0.01	0.00
	99.9	100.2	99.8	100.4	99.5	100.1	99.9	100.1

GGU No. .	132012	132014	132015	81248	81234	84423*	84480	84484*
Zone	5 UM	5	5	4	8 UM	3–4 UM	4	6 UM
SiO_2.....	54.2	52.9	53.2	51.8	55.2	53.9	52.0	54.9
TiO_2.....	0.02	0.01	0.01	0.00	0.11	0.01	0.01	0.12
Al_2O_3.....	3.10	2.84	3.85	3.70	3.01	2.95	5.72	2.05
Cr_2O_3.....	0.03	0.01	0.03	0.00	0.09	0.02	0.00	0.04
FeO	12.8	17.9	16.2	17.2	9.2	11.8	14.4	11.8
MnO	0.31	0.34	0.32	0.31	0.22	0.33	0.20	0.37
MgO.....	29.5	25.2	26.3	25.9	32.3	30.6	26.5	29.9
NiO	nd	nd	nd	0.05	0.10	0.01	0.04	nd
CaO	0.41	0.27	0.18	0.23	0.40	0.49	0.36	0.41
Na_2O	0.01	0.01	0.01	0.00	0.00	0.02	0.04	0.01
K_2O	0.01	0.01	0.01	0.00	0.00	0.01	0.01	0.01
	100.4	99.5	100.0	99.2	100.6	100.1	99.4	99.5

* Major elements reduced by 2 %.
nd not detected.

Table 3b. *Orthopyroxene: atomic contents for 6 oxygens*

GGU No. .	132006	84485	84488	84492	84494	84496	84497	132009
Zone	4	2 UM	2 UM	3 UM	3 UM	3–4 UM	3–4 UMC	4
Si.....	1.869	1.974	1.956	1.903	1.909	1.915	1.956	1.945
Al.....	0.131	0.026	0.039	0.097	0.091	0.085	0.044	0.055
Al.....	0.034	0.021		0.034	0.020	0.032	0.013	0.046
Ti.....	0.000	0.001	0.003	0.001	0.001	0.000	0.002	0.000
Cr.....	0.001	0.001	0.003	0.000	0.003	0.003	0.005	0.000
Mg.....	1.509	1.500	1.549	1.541	1.542	1.586	1.688	1.365
Ni.....	0.002	nd	0.002	0.001	0.001	0.001	0.002	nd
Fe	0.459	0.443	0.430	0.428	0.435	0.372	0.281	0.567
Mn.....	0.009	0.017	0.011	0.010	0.010	0.007	0.002	0.011
Ca	0.30	0.016	0.025	0.014	0.020	0.021	0.015	0.014
Na	0.002	0.000	0.001	0.001	0.001	0.001	0.001	0.0
K.....	0.000	0.001	0.001	0.001	0.001	0.001	0.000	0.000
ΣM	2.036	2.000	2.025	2.031	2.034	2.024	2.009	2.003
ΣT	2.000	2.000	1.995	2.000	2.000	2.000	2.000	2.000
Mg.....	75.5	76.5	77.3	77.6	77.2	80.1	85.2	70.2
Fe	23.0	22.6	21.5	21.6	21.8	18.8	14.1	29.1
Ca	1.5	0.8	1.2	0.8	1.0	1.1	0.8	0.7

GGU No. .	132012	132014	132015	81248	81234	84423	84480	84484
Zone	5 UM	5	5	4	8 UM	3–4 UM	4	6 UM
Si.....	1.920	1.936	1.917	1.899	1.920	1.909	1.876	1.951
Al.....	0.080	0.064	0.083	0.101	0.080	0.091	0.124	0.049
Al.....	0.049	0.058	0.080	0.059	0.043	0.032	0.119	0.037
Ti.....	0.001	0.000	0.000	0.000	0.003	0.000	0.000	0.003
Cr.....	0.001	0.000	0.001	0.000	0.002	0.001	0.000	0.001
Mg.....	1.558	1.374	1.413	1.415	1.674	1.616	1.425	1.584
Ni.....	nd	nd	nd	0.001	0.003	0.000	0.001	nd
Fe	0.379	0.548	0.488	0.527	0.267	0.349	0.434	0.350
Mn.....	0.009	0.010	0.010	0.010	0.006	0.010	0.006	0.011
Ca	0.016	0.011	0.0007	0.009	0.015	0.019	0.014	0.016
Na	0.001	0.001	0.001	0.000	0.000	0.001	0.003	0.001
K.....	0.001	0.001	0.001	0.000	0.000	0.001	0.001	0.001
ΣM	2.015	2.003	2.001	2.011	2.013	1.999	2.003	2.004
ΣT	2.000	2.000	2.000	2.000	2.000	2.000	2.000	2.000
Mg.....	79.8	71.1	74.0	72.5	85.7	81.4	76.1	81.3
Fe	19.4	27.3	25.6	27.0	13.6	17.6	23.2	17.9
Ca	0.8	0.6	0.4	0.5	0.8	1.0	0.7	0.8

nd not detected.

Table 4a. *Diopside: reconaissance microprobe analyses*

GGU No. .	132007	84485	84487	84488*	84490*	84493	84495	132016	84484*
Zone	2 UM	2 UM	2 UM	2 UM	2 UM	3	3	6	6 UM
SiO_2.....	53.4	54.4	54.1	50.1	54.6	52.5	52.5	52.5	52.4
TiO_2.....	0.11	0.08	0.12	0.28	0.09	0.05	0.07	0.13	0.35
Al_2O_3.....	0.86	0.97	0.71	1.11	0.72	1.63	1.85	2.20	2.14
Cr_2O_3.....	0.11	0.03	0.14	0.56	0.05	0.03	0.02	0.04	0.02
FeO.....	4.15	4.70	4.33	9.01	4.41	8.24	8.63	8.62	3.78
MnO	0.16	0.21	0.29	0.12	0.14	0.22	0.18	0.21	0.14
MgO.....	17.2	16.5	17.1	17.7	17.0	13.6	13.8	13.3	16.2
NiO.....	0.02	nd	nd	0.07	0.00	nd	nd	nd	nd
CaO.....	23.3	24.0	24.3	21.7	23.1	22.4	22.6	23.3	24.0
Na_2O.....	0.08	0.08	0.08	0.04	0.07	0.29	0.36	0.33	0.15
K_2O.....	0.0	0.01	0.01	0.01	0.02	0.01	0.01	0.0	0.0
	99.4	100.9	101.1	100.8	100.0	99.1	100.1	100.6	99.4

* major elements reduced by 3 %.
nd not detected.

Table 4b. *Diopside: atomic contents for 6 oxygens*

GGU No. ..	132007	84485	84487	84488	84490	84493	84495	132016	84484
Zone	2 UM	2 UM	2 UM	2 UM	2 UM	3	3	6	6 UM
Si.....	1.967	1.976	1.964	1.872	1.990	1.973	1.958	1.953	1.936
Al.....	0.033	0.024	0.030	0.049	0.010	0.027	0.042	0.047	0.064
Al.....	0.004	0.017			0.021	0.045	0.039	0.049	0.029
Ti.....	0.003	0.002	0.003	0.008	0.002	0.001	0.002	0.004	0.010
Cr.....	0.003	0.001	0.004	0.016	0.001	0.001	0.001	0.001	0.001
Mg.....	0.944	0.894	0.925	0.985	0.923	0.762	0.767	0.737	0.892
Ni.....	0.001	nd	nd	0.002	nd	nd	nd	nd	nd
Fe	0.128	0.143	0.131	0.281	0.134	0.259	0.269	0.257	0.117
Mn.....	0.005	0.006	0.009	0.004	0.004	0.007	0.006	0.007	0.004
Ca	0.919	0.934	0.945	0.868	0.902	0.902	0.903	0.928	0.950
Na.....	0.006	0.006	0.006	0.003	0.005	0.021	0.026	0.024	0.011
K.....	0.000	0.001	0.001	0.001	0.001	0.001	0.001	0.000	0.000
ΣM	2.009	2.004	2.024	2.168	1.993	1.999	2.014	2.007	2.104
ΣT.....	2.000	2.000	1.994	1.921	2.000	2.000	2.000	2.000	2.000
Mg.....	47.4	45.3	46.2	46.1	47.1	39.6	39.5	38.4	45.5
Fe	6.4	7.3	6.5	13.2	6.8	13.5	13.9	13.4	6.0
Ca	46.2	47.4	47.2	40.7	46.0	46.9	46.5	48.3	48.5

nd not detected.

Table 5a. *Hornblende: reconnaissance microprobe analyses*

GGU No. .	132006	132007	84485	84488*	84490*	84491†	84492*
Zone	4	2 UM	2 UM	2 UM	2 UM	3	3 UM
SiO_2.....	44.9	51.1	51.1	46.0	50.6	47.0	46.1
TiO_2.....	0.11	0.46	0.34	0.75	0.45	0.6	0.28
Al_2O_3.....	14.1	6.06	7.35	9.89	7.02	12.0	11.4
Cr_2O_3.....	0.11	0.58	0.20	0.48	0.29	0.03	0.0
FeO	7.68	5.70	6.78	7.41	6.98	13.4	7.96
MnO	0.14	0.08	0.12	0.08	0.11	0.19	0.11
MgO.....	16.3	20.4	18.8	17.8	18.8	11.9	17.1
NiO	0.05	0.14	nd	0.16	0.07	nd	0.10
CaO	12.1	12.4	12.5	12.8	12.6	12.4	12.3
Na_2O	1.69	0.88	0.88	1.65	1.15	0.8	1.21
K_2O.....	0.15	0.14	0.22	0.42	0.37	0.9	0.18
	97.5	98.0	98.4	97.5	98.5	99.2	96.8

GGU No. .	84493	84494*	84495	84496*	84497*	84498	132008	132009
Zone	3	3 UM	3	3–4 UM	3–4 UMC	3–4 C	3–4 C	4
SiO_2.....	47.1	46.9	47.1	48.4	49.1	43.6	47.1	47.2
TiO_2.....	0.56	0.10	0.62	0.14	0.38	0.47	0.61	0.32
Al_2O_3.....	9.88	11.7	10.1	10.8	9.14	15.4	10.6	11.8
Cr_2O_3.....	0.02	0.19	0.07	0.34	0.85	1.64	0.73	0.05
FeO	12.9	7.74	11.8	6.74	4.96	8.27	11.2	9.36
MnO	0.14	0.12	0.1	0.10	0.10	0.11	0.15	0.13
MgO.....	13.4	17.0	13.7	18.1	18.9	13.9	13.8	15.5
NiO	nd	0.05	nd	0.05	0.08	nd	nd	nd
CaO	11.6	12.6	12.1	12.6	12.1	12.6	12.2	12.0
Na_2O	0.88	1.07	0.93	1.28	1.29	1.57	0.90	1.40
K_2O.....	0.60	0.20	0.83	0.29	0.29	0.68	0.99	0.23
	97.1	97.7	97.4	98.9	97.2	98.3	98.4	98.1

GGU No. .	132012	132014	132015	132016	132018†	132020	132021	132022
Zone	5 UM	5	5	6	6	7 C	7	7 C
SiO_2.....	47.8	47.8	46.7	49.0	48.7	44.4	43.7	43.5
TiO_2.....	0.14	0.17	0.26	0.66	0.34	1.28	1.35	1.32
Al_2O_3.....	11.3	11.9	12.7	7.9	11.1	13.9	12.8	15.3
Cr_2O_3.....	0.07	0.08	0.08	0.10	0.01	1.71	0.09	2.24
FeO	6.94	8.96	9.08	14.1	11.0	8.52	16.1	6.78
MnO	0.12	0.15	0.14	0.14	0.16	0.15	0.19	0.07
MgO.....	17.5	16.1	15.9	13.2	15.0	13.7	10.3	14.4
NiO	0.05	nd	nd	nd	nd	nd	nd	nd
CaO	12.5	11.0	10.6	12.3	10.7	12.2	11.6	12.6
Na_2O	0.99	1.25	1.22	0.55	1.07	1.51	1.33	2.04
K_2O.....	0.16	0.10	0.18	0.44	0.14	0.55	0.77	0.49
	97.6	97.5	96.9	98.4	98.2	98.0	98.2	98.8

(continued)

Table 5a (cont.). *Hornblende: reconnaissance microprobe analyses*

GGU No. .	132023	132024	132025	132026	132028	132029	84500	81248
Zone	7	7 C	7	7	7 C	7 C	8 UM	4
SiO_2.....	44.0	42.6	43.2	42.5	44.3	43.3	45.6	44.5
TiO_2.....	1.69	0.83	1.47	1.15	0.65	1.25	0.78	0.24
Al_2O_3.....	11.7	15.0	11.4	13.5	12.9	12.2	13.2	14.6
Cr_2O_3.....	0.11	1.15	0.02	0.19	1.48	1.49	0.0	0.01
FeO.....	12.3	9.13	15.0	15.2	10.1	12.3	6.89	9.6
MnO	0.17	0.19	0.23	0.30	0.18	0.18	0.11	0.12
MgO.....	12.2	13.5	11.0	10.5	13.6	12.4	17.3	15.3
NiO	nd	nd	nd	0.04	0.10	nd	0.05	0.07
CaO.....	12.4	12.1	12.3	10.8	11.7	11.3	12.2	11.5
Na_2O.....	1.16	1.68	1.13	1.55	1.34	1.37	1.86	1.91
K_2O.....	1.36	0.47	0.97	0.63	0.53	0.63	0.34	0.33
	97.3	96.8	96.8	96.3	97.0	96.5	98.4	98.3

GGU No. .	81235	81234	81244	81233	84423*	84480	84484*
Zone	8	8 UM	8	8	3–4 UM	4	6 UM
SiO_2.....	42.3	47.1	42.6	42.3	49.8	44.0	49.5
TiO_2.....	1.09	0.91	1.35	1.98	0.26	0.12	0.78
Al_2O_3.....	12.7	11.7	13.9	12.1	9.28	16.0	9.61
Cr_2O_3.....	0.01	0.33	0.06	0.02	0.10	0.01	0.22
FeO.....	15.9	5.81	13.1	16.6	6.61	7.96	6.05
MnO	0.22	0.06	0.10	0.22	0.09	0.11	0.07
MgO.....	10.4	18.1	12.3	9.65	18.5	15.2	18.1
NiO	0.08	0.10	0.03	0.0	0.01	nd	nd
CaO.....	11.6	13.0	11.3	11.4	13.1	11.5	12.9
Na_2O.....	1.36	1.36	1.71	1.38	0.63	2.09	1.05
K_2O.....	0.68	0.21	0.62	0.78	0.14	0.21	0.09
	96.5	98.7	97.1	96.5	98.5	97.5	98.4

* major elements reduced by 1 %.
† lower accuracy.
nd not detected.

Table 5b. *Hornblende: atomic contents for 23 oxygens*

GGU No. .	132006	132007	84485	84488	84490	84491	84492
Zone	4	2 UM	2 UM	2 UM	2 UM	3	3 UM
Si.....	6.430	7.172	7.161	6.625	7.118	6.761	6.645
Al.....	1.570	0.818	0.839	1.375	0.882	1.239	1.355
Al.....	0.810	0.184	0.375	0.304	0.282	0.795	0.582
Ti.....	0.012	0.049	0.036	0.081	0.048	0.065	0.030
Cr.....	0.012	0.064	0.022	0.055	0.032	0.003	0.0
Mg.....	3.480	4.268	3.927	3.821	3.942	2.551	3.674
Ni	0.006	0.016	nd	0.018	0.008	nd	0.012
Fe	0.919	0.669	0.794	0.892	0.821	1.611	0.959
Mn.....	0.017	0.009	0.014	0.010	0.013	0.023	0.013
Na	0.469	0.239	0.239	0.461	0.314	0.223	0.338
Ca	1.857	1.865	1.877	1.975	1.899	1.911	1.900
K.....	0.027	0.025	0.039	0.077	0.066	0.165	0.033
ΣX.....	2.353	2.129	2.155	2.513	2.269	2.299	2.271
ΣY.....	5.256	5.259	5.168	5.181	5.146	5.048	5.270
% Mg	78.8	86.3	82.9	80.9	82.6	60.8	79.1
% K	1.1	1.2	1.8	3.1	2.9	7.2	1.5
% Na.....	19.9	11.2	11.1	18.3	13.9	9.7	14.9

GGU No. .	84493	84494	84495	84496	84497	84498	132008	132009
Zone	3	3 UM	3	3–4 UM	3–4 UMC	3–4 UMC	3–4 C	4
Si.....	6.897	6.680	6.863	6.781	6.937	6.257	6.798	6.734
Al.....	1.103	1.320	1.137	1.219	1.063	1.743	1.202	1.266
Al.....	0.602	0.644	0.598	0.564	0.458	0.862	0.601	0.718
Ti.....	0.062	0.011	0.068	0.015	0.040	0.051	0.066	0.034
Cr.....	0.002	0.021	0.008	0.038	0.095	0.186	0.083	0.006
Mg.....	2.925	3.609	2.976	3.780	3.980	2.973	2.969	3.296
Ni.....	nd	0.006	nd	0.006	0.009	nd	nd	nd
Fe	1.579	0.922	1.437	0.789	0.586	0.992	1.351	1.116
Mn.....	0.017	0.014	0.012	0.012	0.012	0.013	0.018	0.016
Na	0.250	0.295	0.263	0.348	0.353	0.437	0.252	0.387
Ca	1.820	1.923	1.889	1.891	1.831	1.937	1.887	1.834
K.....	0.112	0.036	0.154	0.052	0.052	0.124	0.182	0.042
ΣX.....	2.182	2.254	2.206	2.291	2.236	2.498	2.321	2.263
ΣY.....	5.187	5.227	5.099	5.204	5.180	5.077	5.088	5.186
% Mg	64.7	79.0	67.2	82.5	86.9	74.7	68.4	74.4
% K	5.1	1.5	7.0	2.3	2.3	5.0	7.9	1.9
% Na.....	11.5	13.1	11.9	15.2	15.8	17.5	10.9	17.1

(continued)

Table 5b (cont.) *Hornblende: atomic contents for 23 oxygens*

GGU No. .	132012	132014	132015	132016	132018	132020	132021	132022
Zone	5 UM	5	5	6	6	7 C	7	7 C
Si	6.773	6.800	6.696	7.104	6.922	6.387	6.470	6.188
Al	1.227	1.200	1.304	0.896	1.078	1.613	1.530	1.812
Al	0.660	0.795	0.842	0.444	0.781	0.744	0.704	0.753
Ti	0.015	0.018	0.028	0.072	0.036	0.138	0.150	0.141
Cr	0.008	0.009	0.009	0.011	0.001	0.194	0.010	0.252
Mg	3.693	3.414	3.398	2.852	3.178	2.938	2.273	3.053
Ni	0.006	nd	nd	nd	nd	nd	nd	nd
Fe	0.822	1.066	1.088	1.709	1.307	1.025	1.993	0.806
Mn	0.014	0.018	0.017	0.017	0.019	0.018	0.024	0.008
Na	0.271	0.345	0.339	0.155	0.295	0.421	0.382	0.563
Ca	1.897	1.677	1.628	1.910	1.629	1.880	1.840	1.921
K	0.029	0.018	0.033	0.081	0.025	0.101	0.145	0.089
ΣX	2.197	2.040	2.000	2.146	1.949	2.402	2.367	2.573
ΣY	5.218	5.320	5.380	5.105	5.322	5.057	5.144	5.013
% Mg	81.5	75.9	75.5	62.3	70.5	73.8	53.0	79.0
% K	1.3	0.9	1.6	3.8	1.3	4.2	6.1	3.5
% Na.....	12.3	16.9	16.9	7.2	15.1	17.5	16.1	21.8

GGU No. .	132023	132024	132025	132026	132028	132029	84500	81248
Zone	7	7 C	7	7	7 C	7 C	8 UM	4
Si	6.519	6.235	6.502	6.391	6.479	6.443	6.455	6.375
Al	1.481	1.765	1.498	1.609	1.521	1.557	1.545	1.625
Al	0.562	0.823	0.524	0.784	0.703	0.573	0.657	0.840
Ti	0.188	0.091	0.166	0.130	0.072	0.140	0.083	0.026
Cr	0.013	0.133	0.002	0.023	0.171	0.175	0.000	0.001
Mg	2.694	2.945	2.468	2.354	2.965	2.750	3.649	3.267
Ni	nd	nd	nd	0.005	0.012	nd	0.006	0.008
Fe	1.523	1.117	1.887	1.911	1.235	1.530	0.815	1.150
Mn	0.021	0.024	0.029	0.038	0.022	0.023	0.014	0.015
Na	0.333	0.477	0.330	0.452	0.380	0.395	0.510	0.530
Ca	1.968	1.898	1.983	1.740	1.833	1.802	1.849	1.765
K	0.257	0.088	0.186	0.121	0.099	0.120	0.061	0.060
ΣX	2.558	2.463	2.499	2.313	2.312	2.317	2.420	2.355
ΣY	5.001	5.133	5.076	5.245	5.180	5.191	5.224	5.307
% Mg	63.5	72.0	56.2	54.6	70.2	64.0	81.5	73.6
% K	10.0	3.6	7.4	5.2	4.3	5.2	2.5	2.6
% Na.....	13.0	19.4	13.2	19.5	16.4	17.0	21.1	22.5

(continued)

Table 5b (cont.). *Hornblende: atomic contents for 23 oxygens*

GGU No. .	81235	81234	81244	81233	84423	84480	84484
Zone	8	8 UM	8	8	3–4 UM	4	6 UM
Si.....	6.404	6.606	6.304	6.422	6.966	6.311	6.924
Al.....	1.596	1.394	1.696	1.578	1.034	1.689	1.076
Al.....	0.670	0.540	0.728	0.587	0.496	1.016	0.508
Ti.....	0.124	0.096	0.150	0.226	0.027	0.013	0.082
Cr.....	0.001	0.037	0.007	0.002	0.011	0.001	0.024
Mg.....	2.347	3.784	2.713	2.183	3.857	3.249	3.774
Ni.....	0.010	0.011	0.004	0.000	0.001	nd	nd
Fe	2.012	0.681	1.621	2.107	0.773	0.954	0.707
Mn.....	0.028	0.007	0.012	0.028	0.011	0.013	0.008
Na	0.399	0.370	0.491	0.406	0.171	0.581	0.285
Ca	1.881	1.953	1.792	1.854	1.963	1.767	1.933
K.....	0.131	0.038	0.117	0.151	0.025	0.038	0.016
ΣX.....	2.411	2.361	2.400	2.411	2.159	2.386	2.234
ΣY.....	5.192	5.156	5.235	5.133	5.176	5.246	5.103
% Mg	53.5	84.6	61.5	50.6	83.1	77.1	84.1
% K	5.4	1.6	4.9	6.3	1.2	1.6	0.7
% Na.....	16.6	15.7	20.4	16.8	7.9	24.3	12.8

nd not detected.

Table 6a. *Phlogopite: reconnaissance microprobe analyses*

GGU No. .	132008	132020	132023	132024	132028	132029	81244	84428
Zone	3–4 C	7 C	7	7 C	7 C	7 C	8	8
SiO_2.....	37.5	37.9	35.8	38.1	37.9	36.9	37.1	37.0
TiO_2.....	2.16	2.76		1.90	2.72	3.81	2.89	1.23
Al_2O_3.....	16.1	17.3	16.1	17.3	16.7	16.1	16.4	19.2
Cr_2O_3.....	0.79	1.18		0.94	1.14	1.05	0.05	0.01
FeO	12.7	5.89	14.2	6.73	9.93	12.9	12.8	10.4
MnO	0.06	0.02		0.03	0.02	0.03	0.02	0.01
MgO.....	15.6	20.1	14.5	20.2	17.6	15.4	16.4	17.6
NiO	nd	0.01		nd	0.18	0.11	0.05	0.05
CaO	0.22	0.16		0.21	0.14	0.10	0.06	0.03
Na_2O	0.04	0.29		0.45	0.26	0.14	0.19	0.34
K_2O	8.99	9.16	7.77	8.77	9.28	9.52	9.00	9.41
	94.2	94.8		94.6	95.8	96.1	95.1	95.2

nd not detected.

Table 6b. *Phlogopite: atomic contents for 22 oxygens*

GGU No.	132008	132020	132024	132028	132029	81244	84428
Zone	3–4 C	7 C	7 C	7 C	7 C	8	8
Si	5.609	5.445	5.487	5.493	5.433	5.486	5.386
Al	2.391	2.555	2.513	2.507	2.567	2.514	2.614
Al	0.447	0.374	0.423	0.346	0.227	0.344	0.680
Ti	0.243	0.298	0.206	0.295	0.422	0.321	0.135
Cr	0.093	0.134	0.107	0.131	0.122	0.006	0.001
Fe	1.513	0.707	0.810	1.203	1.588	1.582	1.266
Mn	0.008	0.002	0.004	0.002	0.004	0.002	0.001
Mg	3.478	4.304	4.336	3.802	3.380	3.614	3.818
Ni	nd	0.001	nd	0.021	0.013	0.006	0.006
Ca	0.035	0.025	0.032	0.022	0.016	0.009	0.005
Na	0.012	0.081	0.126	0.073	0.040	0.054	0.096
K	1.715	1.679	1.611	1.716	1.788	1.698	1.747
ΣX	1.762	1.785	1.769	1.811	1.844	1.761	1.848
ΣY	5.782	5.820	5.886	5.800	5.756	5.875	5.907
% Mg	69.0	85.9	84.2	75.9	68.0	69.5	65.0
% K	97.3	94.0	91.0	94.7	97.0	96.4	94.5

nd not detected.

Table 7. *Plagioclase: reconnaissance microprobe analyses (mol %)*

GGU No.	132006	84491	84493	84495	84498	132008	132009	132014
Or	nd	0.3	0.2	0.2	0.0	0.3	0.04	0.03
Ab	3.6	19.5	11.2	16.4	3.6	22.3	8.1	6.5
An	96.4	80.2	88.4	83.4	96.4	77.4	91.9	93.5

GGU No.	132015	132016	132018	132020*	132021	132022	132023†	132024
Or	0.0	0.0	0.01	0.07	0.25	0.04	0.3	nd
Ab	6.5	9.4	12.2	13.4	12.4	10.8	14–23	10.4
An	93.5	90.6	87.8	86.5	87.4	89.1	86–77	89.5

GGU No.	132025	132028	132029†	81248	81235	81244	81233	84480
Or	nd	nd	0.5	nd	nd	nd	nd	nd
Ab	14.4	15.0	40–52	8.5	14.2	18.6	17.6	4.4
An	85.6	85.0	60–48	91.5	85.8	81.4	82.4	95.6

* Fe 0.05; Mg, Ba, Ti less than 0.01 wt. %.
† Normal zoning.
nd not detected.

Table 8a. *Spinel: reconnaissance microprobe analyses*

GGU No.	84496	81234	84423	84494	132012	84500
Zone	3–4 UM	8 UM	3–4 UM	3 UM	5 UM	8 UM
SiO_2.....	0.84	0.54	0.94	0.81	0.12	0.63
TiO_2.....	0.01	0.02	0.03	0.0	0.0	0.07
Al_2O_3.....	52.4	53.8	56.0	55.9	61.5	61.6
Cr_2O_3.....	7.29	6.83	3.25	3.08	1.36	0.13
FeO.....	23.0	19.6	18.9	24.6	19.6	18.9
MnO	0.18	0.17	0.23	0.18	0.14	0.15
NiO	0.35	0.58	0.44	0.27	0.34	0.22
MgO.....	15.0	17.0	16.7	14.4	15.9	17.6
CaO.....	0.21	0.10	0.22	0.22	0.05	0.09
	99.4	98.6	96.6	99.4	98.9	99.3

Arranged in order of decreasing Cr content.

Table 8b. *Spinel: atomic contents for 32 oxygens*

GGU No. ...	84496	81234	84423	84494	132012	84500	Apollo 14
Zone	3–4 UM	8 UM	3–4 UM	3 UM	5 UM	8 UM	(STEELE, 1972)
Si.....	0.182	0.116	0.204	0.174	0.025	0.130	0.03– 0.27
Ti.....	0.001	0.004	0.005	0.0	0.0	0.011	0.03– 0.15
Al.....	13.36	13.59	14.23	14.11	15.22	15.03	12.2 –15.2
Cr.....	1.247	1.158	0.554	0.521	0.226	0.021	0.5 – 3.6
Fe^3.....	1.170	1.107	0.962	1.152	0.518	0.788	
Fe^2.....	2.990	2.406	2.445	3.256	2.918	2.483	1.9 – 3.8
Mn.....	0.033	0.031	0.042	0.032	0.025	0.026	0.02– 0.03
Ni.....	0.061	0.097	0.077	0.046	0.056	0.036	
Mg.....	4.833	5.428	5.363	4.595	4.976	5.426	4.1 – 6.4
Ca	0.048	0.023	0.051	0.050	0.011	0.020	0.03– 0.15
ΣX.....	15.96	15.98	15.96	15.96	15.99	15.96	
ΣY.....	7.96	7.99	7.98	7.98	7.99	7.99	

Iron split into ferrous and ferric fractions on arbitrary basis.

Table 9a. *Chromite: reconnaissance microprobe analyses*

GGU No.	84497	84498	132020	132022	132024	132028	132029
Zone	3–4 UMC	3–4 C	7 C	7 C	7 C	7 C	7 C
SiO_2	0.64		0.10		nd	0.03	0.0
TiO_2	0.30		0.31		0.20	0.25	1.56*
Al_2O_3	26.4	36.4	18.8	27.1	24.6	18.0	12.6
Cr_2O_3	26.5	24.3	36.0	35.5	31.2	35.2	30.7
FeO	35.9	32.6	34.3	31.3	36.0	39.3	47.8
MnO	0.34		0.54		0.59	0.57	0.48
NiO	0.23		0.05		nd	0.05	0.02
MgO	7.55	5.16	2.22	4.34	2.82	1.28	0.91
CaO	0.06		0.04		0.10	0.06	0.06
	97.9		92.4		95.5	94.8	94.0

* Varies by factor of 2.
nd not detected.
Arranged in order of increasing height of reconstructed traverse 13.

Table 9b. *Chromite: atomic contents for 32 oxygens*

GGU No.	84497	84498	132020	132022	132024	132028	132029	Bushveld
Zone	3–4 UMC	3–4 C	7 C	7 C	7 C	7 C	7 C	CAMERON (1964)*
Si	0.162		0.029		nd	0.008	0.0	
Ti	0.058		0.067		0.041	0.053	0.341	0.062
Al	7.862	10.56	6.367	8.27	7.845	6.005	4.319	4.510
Cr	5.293	4.73	8.165	7.27	6.675	7.877	7.058	9.734
Fe^3	2.584	0.63	1.348	0.453	1.440	2.030	4.202	1.458
Fe^2	5.000	6.08	6.880	6.326	6.701	7.273	7.420	4.143
Mn	0.073		0.131		0.134	0.137	0.119	0.097
Ni	0.048		0.012		nd	0.012	0.005	
Mg	2.843	1.89	0.949	1.675	1.136	0.539	0.395	3.908
Ca	0.017		0.012		0.029	0.023	0.023	
ΣX	15.96	15.92	15.98	15.99	16.00	15.97	15.92	
ΣY	7.98	7.96	7.98	8.00	8.00	7.98	7.96	

* Leader seam, Farm Jagdlust, Eastern Bushveld complex. Wet chemical analysis.
nd not detected.

Table 10. *Magnetite: reconnaissance microprobe analyses*

GGU No.	132007	84488	84484	84490	84485	84423	84500
Zone	2 UM	2 UM	6 UM	2 UM	2 UM	3–4 UM	8 UM
SiO_2	0.50	0.81	0.75	0.69	0.81	0.67	0.39
TiO_2	3.11	3.18	2.49	2.03	2.45	0.43	1.51
Al_2O_3	3.88	3.20	2.94	2.31	1.79	1.08	1.31
Cr_2O_3	13.45	9.87	9.39	6.56	4.71	0.87	0.13
FeO, Fe_2O_3*	~ 76	~ 80	~ 82	~ 86	~ 89	~ 95	~ 96
MnO	0.40	0.33	0.39	0.31	0.30	0.14	0.14
NiO	0.39	0.56	0.34	0.22	0.25	0.22	0.11
MgO	1.63	1.25	1.16	1.02	0.78	0.90	0.91
CaO	0.22	0.07	0.40	0.27	0.29	0.15	0.11

* Estimated by difference.
Arranged in order of decreasing Cr.

REFERENCES

Black, L. P., Moorbath, S., Pankhurst, R. J. & Windley, B. F. 1973: $^{207}Pb/^{206}Pb$ whole rock age of the Archan granulite facies metamorphic event in West Greenland. *Nature, Phy. Sci.* **244**, 50–53.

Boyd, F. R. 1970: Garnet peridotites and the system $CaSiO_3$-$MgSiO_3$-Al_2O_3. *Miner. Soc. Amer. Spec. Pap.* **3**, 63–75.

Boyd, F. R. & England, J. L. 1964: The system enstatite-pyrope. *Carnegie Inst. Washington Year Book* **63**, 157–161.

Cameron, E. N. 1964: Chromite deposits of the eastern part of the Bushveld Complex. *in* Haughton, S. H. (edit.). *The geology of some ore deposits of South Africa*, **2**, 131–168.

Dawson, J. B., Powell, D. G. & Reid, A. M. 1970: Ultrabasic xenoliths and lava from the Lashaine volcano, northern Tanzania. *J. Petrology*, **11**, 519–548.

Deer, W. A., Howie, R. A. & Zussman, J. 1963: Rock-forming minerals. 5 vols. London: Longmans.

Ernst, W. G. 1968: *Amphiboles*. New York: Springer-Verlag.

Frisch, T. 1971: Chemical data on some rock-forming minerals from high-grade gneisses, amphibolites and anorthosites from the Fiskenæsset area. *Rapp. Grønlands geol. Unders.* **35**, 22–23.

Ghisler, M. & Windley, B. F. 1967: The chromite deposits of the Fiskenæsset region, West Greenland. *Rapp. Grønlands geol. Unders.* **12**, 38 pp.

Howie, R. A. & Smith, J. V. 1966: X-ray emission microanalysis of rock-forming minerals. V. Orthopyroxenes. *J. Geol.* **74**, 443–462.

Howie, R. A. & Subramaniam, A. P. 1957: The paragenesis of garnet in charnockite, enderbite, and related granulites. *Mineralog. Mag.* **31**, 565–586.

Kostyuk, E. A. & Sobolev, V. S. 1969: Paragenetic types of calciferous amphiboles of metamorphic rocks. *Lithos* **2**, 67–81.

KRETZ, R. 1960: The distribution of certain elements among coexisting calcic pyroxenes, calcic amphiboles and biotites in skarns. *Geochim. Cosmochim. Acta* **20**, 161–191.

— 1963: Distribution of magnesium and iron between orthopyroxene and calcic pyroxene in natural mineral assemblages. *J. Geol.* **71**, 773–785.

LEAKE, B. E. 1968: A catalog of analyzed calciferous and sub-calciferous amphiboles together with their nomenclature and associated minerals. *Geol. Soc. Amer. Spec. Pap.* **98**, 210 pp.

RUCKLIDGE, J. 1967: A computer program for processing microprobe data. *J. Geol.* **75**, 126 only.

SIMKIN, T. & SMITH, J. V. 1970: Minor-element distribution in olivine. *J. Geol.* **78**, 304–325.

SMITH, J. V. 1965: X-ray emission analyses of rock-forming minerals. I. Experimental techniques. *J. Geol.* **73**, 830–864.

— 1966: X-ray emission microanalysis of rock-forming minerals. II. Olivines. *J. Geol.* **74**, 1–16.

STEELE, I. M. 1972: Chromian spinels from Apollo 14 rocks. *Earth planet. Sci. Lett.* **14**, 190–194.

WINDLEY, B. F., HERD, R. K. & BOWDEN, A. A. 1973: The Fiskenæsset complex, West Greenland. Part I. A preliminary study of the stratigraphy, petrology, and whole-rock chemistry from Qeqertarssuatsiaq. *Bull. Grønlands geol. Unders.* **106** (also *Meddr Grønland* **196**[2]), 40 pp.

B. F. WINDLEY
Department of Geology
Bennett Building. The University
Leicester
England

J. V. SMITH
Department of the Geophysical Sciences
University of Chicago
5734 Ellis Avenue
Chicago
Illinois 60637
U. S. A.

Færdig fra trykkeriet den 18. januar 1974.